



PHOTOVOLTAIC PROPERTIES OF POLYMER BASED  
BULK HETEROJUNCTION SOLAR CELL COMPOSED  
OF POLY[3-(2,5-DIOCTYLE-PHENEYL)  
THIOPHENE](PDOPT) AND (PCBM)

By

Tizazu Masresha

SUBMITTED IN PARTIAL FULFILLMENT OF THE  
REQUIREMENTS FOR THE DEGREE OF  
MASTER OF SCIENCE

AT

ADDIS ABABA UNIVERSITY

ADDIS ABABA, ETHIOPIA

JULY 2006

ADDIS ABABA UNIVERSITY  
DEPARTMENT OF  
PHYSICS

The undersigned hereby certify that they have read and recommend to the Faculty of Science for acceptance a thesis entitled “**Photovoltaic Properties of Polymer based bulk heterojunction Solar cell composed of poly[3-(2,5-dioctyle-pheneyl) thiophene](PDOPT) and (PCBM)**” by **Tizazu Masresha** in partial fulfillment of the requirements for the degree of **Master of Science**.

Dated: July 2006

Supervisor:

\_\_\_\_\_  
Dr. Genene Tessema

Examiners:

\_\_\_\_\_  
Dr. Tesgera Bedassa

\_\_\_\_\_  
Dr. Mebratu G/Mariam

ADDIS ABABA UNIVERSITY

Date: **July 2006**

Author: **Tizazu Masresha**

Title: **Photovoltaic Properties of Polymer based bulk heterojunction Solar cell composed of poly[3-(2,5-dioctyle-pheneyl) thiophene](PDOPT) and (PCBM)**

Department: **Physics**

Degree: **M.Sc.** Convocation: **July** Year: **2006**

Permission is herewith granted to Addis Ababa University to circulate and to have copied for non-commercial purposes, at its discretion, the above title upon the request of individuals or institutions.

---

Signature of Author

THE AUTHOR RESERVES OTHER PUBLICATION RIGHTS, AND NEITHER THE THESIS NOR EXTENSIVE EXTRACTS FROM IT MAY BE PRINTED OR OTHERWISE REPRODUCED WITHOUT THE AUTHOR'S WRITTEN PERMISSION.

THE AUTHOR ATTESTS THAT PERMISSION HAS BEEN OBTAINED FOR THE USE OF ANY COPYRIGHTED MATERIAL APPEARING IN THIS THESIS (OTHER THAN BRIEF EXCERPTS REQUIRING ONLY PROPER ACKNOWLEDGEMENT IN SCHOLARLY WRITING) AND THAT ALL SUCH USE IS CLEARLY ACKNOWLEDGED.

*To My mother Enanni Kassaye*  
*and*  
*My father Masresha Alemu*

# Table of Contents

Table of Contents	v
List of Tables	vii
List of Figures	viii
Abstract	xii
Acknowledgements	1
<b>1 Introduction</b>	<b>1</b>
<b>2 Chemistry and Physics of Conjugated Polymers</b>	<b>5</b>
2.1 Bonding( $\pi$ -and $\sigma$ -bonds)	5
2.2 Electronic structure of Conjugated polymers	8
2.2.1 Theoretical understanding of the existence of band gap in conducting polymers	11
<b>3 Quasi-particles</b>	<b>15</b>
3.1 Doping in conducting polymers	22
3.2 charge transport and conductivity in conjugated polymers	25
<b>4 Metal-semiconductor contact(Metal-CP contact)</b>	<b>29</b>
4.1 Current-voltage Characteristics	32
4.2 Impedance spectroscopy and Modelling concept	36
<b>5 Photovoltaic phenomena in conducting polymer devices</b>	<b>40</b>
5.1 Review	40
5.2 Photogeneration of free charge carriers	42
5.2.1 Schottky Junction(Single layer)devices	43

5.2.2	Donor-Acceptor Bilayer Devices . . . . .	46
5.2.3	Bulk heterojunction solar cells . . . . .	48
5.3	Characterization of photovoltaic devices . . . . .	50
<b>6</b>	<b>Experimental</b>	<b>54</b>
6.1	Absorption spectrum measurement . . . . .	54
6.2	Device preparation . . . . .	55
6.3	Device characterization . . . . .	58
6.3.1	Current-Voltage measurement . . . . .	58
6.3.2	Complex impedance measurement . . . . .	58
<b>7</b>	<b>Results and Discussion</b>	<b>59</b>
7.1	Absorption spectra . . . . .	59
7.2	Current density-Voltage ( J-V ) characteristics . . . . .	61
7.3	The Cole-Cole plot . . . . .	67
	<b>Conclusion</b>	<b>70</b>
	<b>Bibliography</b>	<b>72</b>

# List of Tables

7.1	Electrical parameters extracted from the J-V characteristics in the dark	64
7.2	Photovoltaic performance parameters of bulk heterojunction solar cell device under $100mWcm^{-2}$ illumination . . . . .	65
7.3	Parameters obtained from the impedance spectra for the device under test . . . . .	67

# List of Figures

2.1	Energy schematics showing the overlap of the 1s atomic orbital of two H-atoms to form a bonding and anti-bonding molecular orbital. . . .	6
2.2	formation of $\sigma$ -bonds and $\Pi$ -bonds by the overlap of a)1s orbitals and b) $2p_z$ orbitals . . . . .	7
2.3	Combination of molecular orbitals leads to the formation of band . .	9
2.4	Chemical formula of some of the the most significant conjugated polymers. . . . .	10
2.5	$sp^2$ -hybridized orbitals resulting in strong $\sigma$ -bonds along a conjugated segments and $\Pi$ -bonds resulting from $p_z$ orbitals located orthogonally with respect to the the plane of $\sigma$ -bonds. For clarity, the overlap between $p_z$ orbitals is not explicitly shown. . . . .	11
2.6	The formation of a band gap at the border of the first Brillouin zone (a) equal length of the bonds will yield a metallic behavior (b)alternating double and single bonds, with shorter length of the double bonds, compared with single bonds due to Peierls distortion. . . . .	12
3.1	(a) and (b) stands for ground state degeneracy of two phases of dimerised trans-PA (c) a domain wall(soliton) separating the two phases of trans-PA chain . . . . .	16
3.2	(a)Formation of mid gap-state due to the creation of soliton. (b)The anti-bonding form the CB and the VB of the intrinsic conducting polymers (c)The solton band . . . . .	17

3.3	Solitons and electronic states, their charge, spin state, and their corresponding electronic transition . . . . .	18
3.4	The aromatic and Quinoidal form of (a) polythiophene and (b) Cis-polyacetylene . . . . .	19
3.5	Unstability of soliton in non-degenerate polythiophene. . . . .	20
3.6	The four possible states of polythiophene . . . . .	21
3.7	Energy band diagram for (a) hole polaron, (b) electron polaron (c) hole bipolaron (d) electron bipolaron . . . . .	22
3.8	Conductivity of few Organic and Inorganic Materials Adapted from ref.16. . . . .	23
3.9	Doping of Polyacetylene gives polaron . . . . .	24
4.1	The energy band diagram of (a) an isolated metal adjacent to an isolated n-type semiconductor under non equilibrium condition (b) a metal-semiconductor contact in thermal equilibrium . . . . .	30
4.2	The energy band diagram of (a) an isolated metal adjacent to an isolated p-type semiconductor contact under non equilibrium condition (b) metal/p-type semiconductor contact under open circuit condition . . . . .	31
4.3	Energy band diagram of rectifying metal -n-type semiconductor contact at a) thermal equilibrium b) forward bias and c) reverse bias . . . . .	33
4.4	Energy band diagram of Metal/p-type conducting polymer/Metal Schottky barrier under open circuit condition . . . . .	36
4.5	The impedance plotted as a planar vector using rectangular and polar coordinate. . . . .	37
4.6	a) RC-parallel circuit b) Ideal Cole-Cole plot of the impedance of parallel RC circuit. . . . .	38
4.7	a) RC-parallel circuit connected in series with contact resistor b) Its Cole-Cole plot. . . . .	39

5.1	MIM picture for polymer diode under different working conditions (a) Short circuit, under illumination photogenerated charges drift to ward the contacts. (b) Flat band or open circuit under illumination, the $V_{oc}$ is the work function difference between the two contacts, (c) Diode under reverse bias, diode work as photodetector, and (d) Diode under forward bias, diode can work as light emitting diode. . . . .	44
5.2	The interface between two different organic semiconductors can either: (a)facilitate charge transfer (D/A) interface (b)energy transfer forms depends on the position of HOMO and LUMO levels. . . . .	47
5.3	Schematic representation of a polymer thin film photoactive device, made of an electron-acceptor and a hole-transporting (HTL) polymer, with an arbitrary chosen mixing profile, an ITO anode and Al cathode: (TOP) and film cross section: (Bottom) energy diagram . Adapted from ref.30. . . . .	49
5.4	Maximum power rectangle of the solar cell I-V characteristics . . . .	51
6.1	A polymer on the glass substrate prepared for Absorption . . . . .	55
6.2	Diagram showing one-third of ITO is removed ready for spin coating	56
6.3	Finalized solar cell prepared for characterizations, Top: Chemical structure of PDOPT, PEDOT:PSS and PCBM . . . . .	57
7.1	The Absorption spectrum of neutral PDOPT . . . . .	59
7.2	The Absorption spectrum of blend PDOPT:PCBM (1:2 Wt ratio) blend and pure PDOPT . . . . .	60
7.3	Current density-voltage characteristics of bulk heterojunction device of structure ITO/PEDOT:PSS/PDOPT:PCBM/Al . . . . .	61
7.4	Semi-log plot of bulk heterojunction device of structure ITO/PEDOT:PSS/PDOPT:PCBM/Al . . . . .	63
7.5	J-V characteristics of bulk heterojunction device of structure ITO/PEDOT:PSS/ PDOPT:PCBM/Al under illumination of $100mWcm^{-2}$	64

7.6	Cole-Cole plots of bulk heterojunction device of structure ITO/PEDOT:PSS/ PDOPT:PCBM/Al . . . . .	68
7.7	An equivalent circuit for the device under test as model for the Cole- Cole plot of fig 7.6 . . . . .	69

# Abstract

The Theme of this thesis is to characterize polymer based photovoltaic cell using the J-V measurements and impedance spectroscopy. Absorption spectra of pure (neutral) poly[3-(2,5-dioctyle-pheneyl) thiophene](PDOPT) study showed that the optical band gap of this polymer about  $\sim 2\text{eV}$ , indicating that it is in the range of inorganic semiconductors. The sandwich structure ITO/PEDOT:PSS/PDOPT:PCBM/Al were utilized to fabricate the device. All the devices which are tested in this work, are bulk heterojunction that are composed of the p-type , PDOPT and n-type fullerene derivative, (phenyl-(6,6')- $c_{61}$ )-butyric acid methyl ester ( PCBM )blend. The J-V measurements under both illumination dark indicated that the typical diode rectification property with rectification ratio  $1.5 \times 10^3$  at (  $\pm 1.8\text{V}$  ) Such a device of blend ratio 1:2 (PDOPT:PCBM) expected to show a photovoltaic behavior with a power conversion efficiency about 0.028 % under  $100\text{mWcm}^{-2}$ .

# Acknowledgements

I am very much grateful to my advisor, Dr. Genene Tessema for his genuine guidance, professional support and instructive comments with kindly treatment of my work.

I wish to express my gratitude to the department of physics, Addis Ababa University.

I would like to give sincere and deepest gratitude to my brother Wondie Masresha for his brotherly moral encouragement that he imparts to the fulfillment of this study.

Last, but not least, B/G/R Education Bureau for sponsoring me to join the the school of graduate studies.

Addis Ababa University

Tizazu Masresha

July, 2006

# Chapter 1

## Introduction

Materials, which are insulating heat and electricity, are of great technological importance and are, therefore, used in large quantities in the electronics industry, eg., as handles for a variety of tools, as coatings of wires, or for casings of electrical equipment. Most polymeric materials have the required insulating properties and have been used for decades for this purpose. It came, therefore, as a surprise when it was discovered that some polymers and organic substances may have electrical properties which resemble those of conventional semiconductors, metals, or even superconductors[1]. However, the application of polymers for industrial purposes are greatly hampered by the fact that conducting polymers are unstable in air and humidity or above room temperature. Besides, many dopants used to improve conductivity are highly toxic, and doping often makes the polymer brittle. These problems might be overcome, however, as more conducting polymers are synthesized.

Polymers are long chain macromolecules, made of repeating monomeric units, with a large molecular weight ( $> 10,000g/mol$ ). Monomers are the smallest unit of the polymers that repeats itself in polymer chains. The monomer itself can be

anything from a simple molecule, consisting of a few atoms, to a large and complex molecule. For instance, the normal alkane hydrocarbon series methane, ethane etc., are compounds which have the general structure,  $H-(CH_2)_n-H$ , where the number of  $-CH_2-$  groups,  $n$ , is allowed to increase up to several thousands. Generally the number of carbon in the chain ( $n$ ) determines the physical and chemical properties of the polymers, which are composed of the alkane series[2]. Polymers can be categorized into two, namely, non-conjugated and conjugated polymers. Non-conjugated polymers are often characterized by electrically insulating property. Conjugated polymers are class of plastic materials for which metallic and semiconductor characteristics can be observed. These polymers have unsaturated double bonds separated by saturated single bonds along polymer back bone and they are materials with a wealth of potential applications.

Conjugated polymers become highly conducting ( and can reach a metallic conductivity regime ) when oxidized or reduced a process called doping. The main focus of the early research activity on conducting polymers was on their electrical conductivity. Neutral( undoped ) conjugated polymers are insulators or semiconductors. To make these polymers electrically conducting, one should introduce species, which are electron accepting ( oxidizing agents ) or electron donating ( reducing agents ). However, the process of doping in conducting polymers is different from that of conventional semiconductors. In semiconductors doping involves replacing some of the atoms with atoms that have either more or less electrons while in conducting polymers the dopant molecules never replace any of the atoms of the polymers; rather they simply act as associates that accept or donate electrons[3]. By appropriately adjusting

the doping level, conductivity anywhere between that of the undoped (insulating or semiconducting) and that of fully doped (metallic) forms of the conjugated polymer may be achieved.

Clearly, inorganic semiconductors have worked just excellent for several decades. However, organic materials offer several advantages over their inorganic and traditional counterparts[4,5]. Some of the potential benefits are:

**Low weight** : The density of molecular materials and polymers are much lower than those of traditional metals (  $1 - 2g/cm^3$  compared to  $3 - 10g/cm^3$  )

**Low cost** : Traditional semiconductors are extremely sensitive to impurities and must be produced, handled in high-tech clean rooms. Organic materials, on the other hand, may be synthesized in relatively unsophisticated laboratories and are much more tolerant to contaminations.

**Tunability** : The art of organic chemistry offers an infinite amount of chemical modification of the active materials, which may be fine tuned to suit each desired application.

**Flexibility** : Inorganic semiconductors are terribly stiff and therefore, useless or less useful for flexible devices. Many organic semiconductors are on the other hand quite flexible, making devices such as plastic color displays realizable.

**Solubility** : many molecular materials are soluble in common organic solvents and can be therefore be applied on to the desired substrates by simple evaporation i.e, organic semiconductors are solution processed. This makes it possible to produce the blends and structures which exhibit the rich photophysics.

This study focuses on the polymer based solar cell devices constructed from a polymer, poly[3-(2,5-dioctyle phenyle)thiophene] with good light absorption ability and hole conductance blended with fullerene derivative PCBM that has high electron affinity.

## Chapter 2

# Chemistry and Physics of Conjugated Polymers

The idea of utilizing organic materials for electronic devices has been the subject of research for several decades. Organic materials are typically inexpensive, easily processable and their functionality by molecular design and chemical synthesis. The development of all the applications has, however, to some extent been limited by low stability and lack of easy processibility. Consequently, a considerable research has effort has been directed toward the design and synthesis awaits ahead[6]. In this respect an understanding the correlation of physical properties with the molecular structure should be given a prime importance because the electrical/electronic properties of polymers depends on the structure of polymers.

### 2.1 Bonding( $\Pi$ -and $\sigma$ -bonds)

Organic compounds often composed of carbon back bone whose molecular structure mainly depends on the valence electrons of carbon. Consider the simplest atom in nature, i.e, the hydrogen; it contains an electron surrounding the hydrogen nucleus. Suppose two hydrogen atoms are brought together to form a molecule. Ofcourse,

there are two possible ways in which the  $1s$  atomic orbital of the hydrogen atom superpose with each other to form a molecular orbital. If the energy of the electrons in molecular orbital is less than the sum of the energies of the  $1s$  electrons in atomic orbital the resulting MO is called bonding molecular orbital. This gives a stable structure of the hydrogen molecule, however, if the energy is greater than the sum of the individual electrons in the atomic state the resulting bond is called anti-bonding molecular orbital. (see Fig 2.1) The binding force which hold the individual atoms

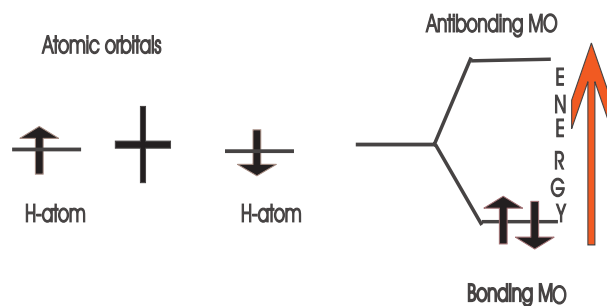


Figure 2.1: Energy schematics showing the overlap of the  $1s$  atomic orbital of two H-atoms to form a bonding and anti-bonding molecular orbital.

(in the hydrogen molecule) together are usually covalent. They are based on the wave function of the two atom electrons overlap, which means that the two electrons will interact. This interaction or perturbation results in the discrete quantized energy level splitting into two discrete energy levels and are responsible for forming a hydrogen molecule from two hydrogen atoms. Quantum mechanics explains covalent bonds by showing that a lower energy state is achieved when two equal atomic systems ( orbitals ) are closely coupled and in this way exchange their energy [1,7,8]. There are two possible geometrical symmetry of a covalent bond. The first kind of

bond is called sigma ( $\sigma$ ) which has cylindrical symmetry about the line joining the two nuclei forming the covalent bond (see fig.2.2). It involves the overlap of end of one orbital with end of the other. Another type of covalent bond can be formed by

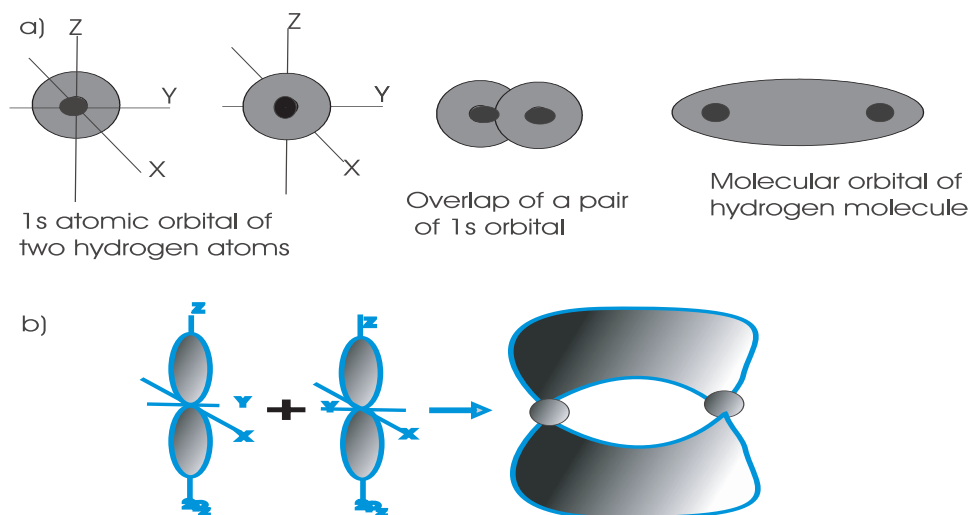


Figure 2.2: formation of  $\sigma$ -bonds and  $\Pi$ -bonds by the overlap of a)1s orbitals and b)2p<sub>z</sub> orbitals

side way the overlap of the adjacent 2P<sub>z</sub> atomic orbitals. This covalent bond of the molecular orbital is not cylindrically symmetric about the line joining the two atoms, the resulting bond is called  $\Pi$ -bond (see fig.2.2). Hence, bonds of organic molecules are combinations of sigma and one or more  $\Pi$ -bonds .

Generally, the  $\sigma$ -electrons are responsible for the strong covalent bond and are localized between the two bonded nuclei. The  $\Pi$ -electrons are also involved in chemical bonding, but they tend to form weaker and less localized bonds, compounds containing  $\Pi$ -electrons are called unsaturated [2].

## 2.2 Electronic structure of Conjugated polymers

The chemical formula of some of the most important organic conducting polymers ( before doping ) are shown in fig.2.4. It can be seen that a common feature is the occurrence of double bonds alternating with single bonds along the polymer chain( conjugated bonds ). The reason that polymers with conjugated bonds form the basis of the organic conducting can be understood as follows. In these polymers, three of the four electrons in the outer shell of a carbon occupy hybridized states from one  $2s$  and two  $2p$  states (  $sp^2$  hybridization ). These electrons form strong  $\sigma$ -bonds that play the key role in forming the structure-in the poly acetylene each carbon atom form these  $\sigma$ -bonds with one hydrogen and the two neighboring carbons. That leaves one valence electron left over ( the  $\Pi$ -electron ), which occupies a  $p_z$ -orbital ( which is not hybridized, is orthogonal to the  $\sigma$ -bonds ). The  $\Pi$ -electron wave functions from different carbon atoms overlap to form a  $\Pi$  -band. In other words, the  $p_z$ -orbital overlaps with another  $p_z$  of the neighboring atoms to form the so called  $\Pi$ -molecular orbital(  $\Pi$ -band ) that spread out over the polymer chain. The lower energy of  $\Pi$ -molecular orbital ( bonding ) form the valence band while the higher energy corresponds to  $\Pi^*$ -molecular orbital ( anti-bonding ). With each delocalized orbital having only one electron, this band would be half-filled and might therefore be expected to be metallic ( because there would be a finite density of states at the fermi level and hence many states available for metallic conduction ). However, the energy of the system is lowered if the  $\Pi$ -electron density is increased between every alternate pair of carbon atoms to form a  $\Pi$ -bond in addition to the  $\sigma$ -bond, i.e., if conjugated bonds are formed as shown in fig 2.4. An energy gap then appears in the middle of the  $\Pi$ -electron band between filled bonding states ( the  $\Pi$ -band ) and

empty anti-bonding states ( the  $\Pi^*$ -band ), lowering the energy of the filled states. For polyacetylene this band gap is approximately 1.7eV, so pristine polyacetylene shows not metallic conductivity but only a very small semiconductor like-conductivity. Thus , the essential structural characteristics of all conjugated polymers is their quasi-infinite  $\Pi$ -system extending over a large number of recurring monomeric units[6,9]. This feature results in materials with directional conductivity, strongest along the axis of the chain.

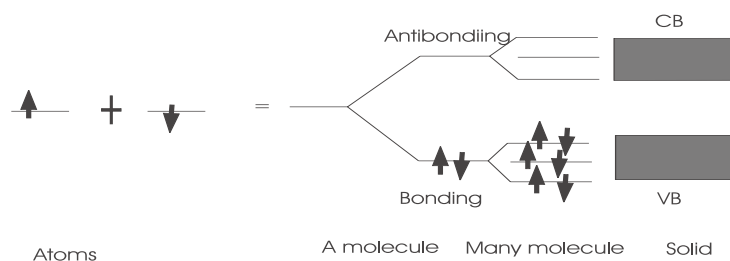


Figure 2.3: Combination of molecular orbitals leads to the formation of band

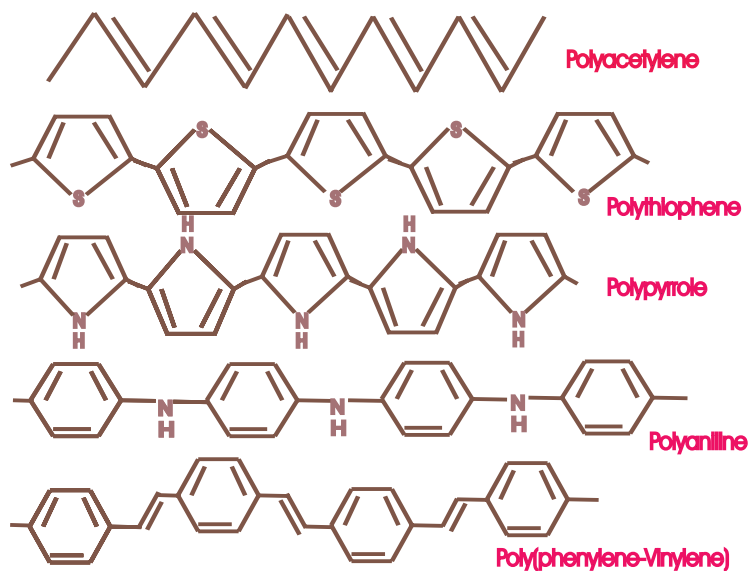


Figure 2.4: Chemical formula of some of the the most significant conjugated polymers.

Electronically conducting polymers are extensively conjugated molecules, and it is believed that they possess a spatially delocalized band like structure. These bands stem from the splitting of interacting molecular orbitals of the constituent monomer units in a manner reminiscent of the band structure of solid state semiconductors ( fig.2.3 ).

The above fig.2.3 shows that as the number of molecular orbitals increases, they get closer together and eventually converge into two bands within which the ( MO ) molecular orbital spacing is so small it can be regarded as a continuum rather than discrete energy levels. The space between the two energy bands is called the band-gap and represents the energy required to promote an electron from the highest occupied molecular orbital ( HOMO ), to the lowest unoccupied molecular orbital ( LUMO ).

## 2.2.1 Theoretical understanding of the existence of band gap in conducting polymers

The conjugated  $\Pi$ -system is responsible for the unique quasi-dimensional electronic and optical properties of polymers. The nature of bandgap in conducting polymers

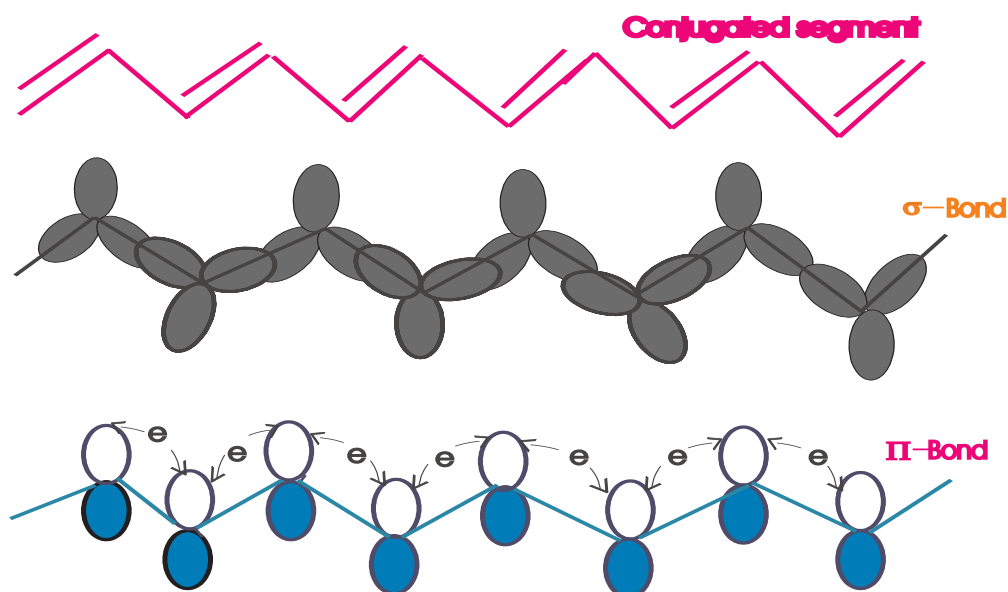


Figure 2.5:  $sp^2$ -hybridized orbitals resulting in strong  $\sigma$ -bonds along a conjugated segments and  $\Pi$ -bonds resulting from  $p_z$  orbitals located orthogonally with respect to the the plane of  $\sigma$ -bonds. For clarity, the overlap between  $p_z$  orbitals is not explicitly shown.

stems from the periodic arrangement of the monomer units which can be regarded as one dimensional system. One dimensional approach theoretical calculations for the motion of electrons in metals produced important information such as band gap and other properties of metals [9]. By treating electrons to be subjected to periodic potentials instead free charged particle in one dimensional lattice; calculation were able to predict the existence of band gap in metals. Analogously, efforts were also

made to understand the origin of band gap in conjugated polymer by considering them as one dimensional system and using the concept of Peierls' distortion [10].

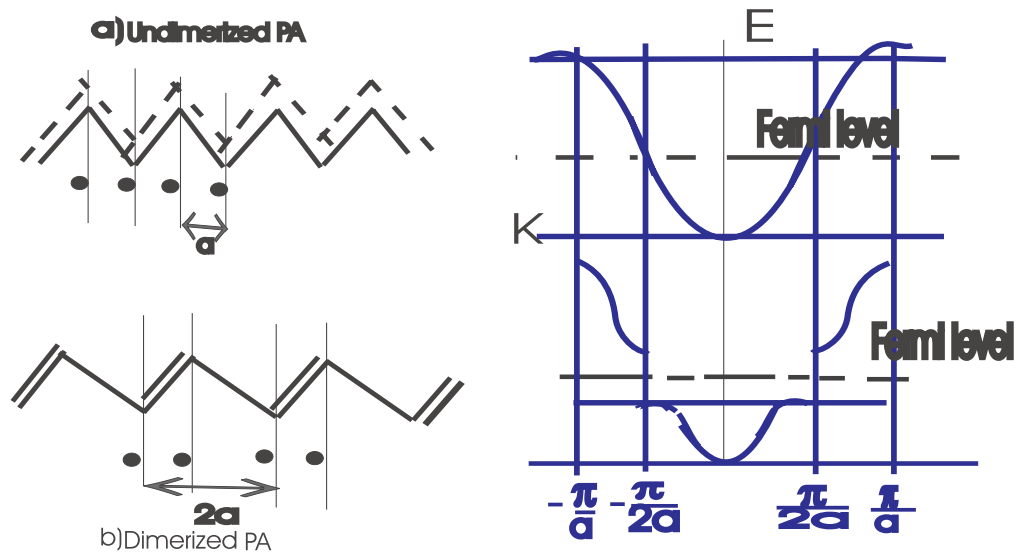


Figure 2.6: The formation of a band gap at the border of the first Brillouin zone (a) equal length of the bonds will yield a metallic behavior (b) alternating double and single bonds, with shorter length of the double bonds, compared with single bonds due to Peierls distortion.

If the bond length between adjacent carbon atoms of the conjugated polymer chain is equidistant, then the unit cell should consist of one carbon atom and one electron ( $\pi$ -electron). This implies that a conjugated polymer would act as a metal, because one electron per unit cell would lead to a partially filled band [12]. This, however, is not the case for conjugated polymers. They are in the neutral state known as semiconducting or insulating, because there is a non-equidistant distance between consecutive atoms. The system will have alternating double and single bonds where the double bond is shorter than the single bond. This results in a unit cell of two carbon atoms and

thus two electrons. A gap at the border of the first Brillouine zone will open up and thus create a band-gap characteristics of semiconducting materials. This is also called Peierls gap after the physicist R.E Peierls, who showed that a one dimensional metal having equidistant bond length would be unstable and the system would be found to be in a dimerised state ( see fig. 2.6 ).

In other words, the dimerised situation in the lower portion of the fig 2.6(b), because organic one-dimensional systems are intrinsically soft, there is a strong inter-connection between the electronic structure and the geometry. However, this " soft " molecule is slightly altered geometrically, a so called a Jahn Teller distortion ( in chemistry ) corresponding to Peierls ( in physics ). In the " distorted " geometry, the  $C - C$  bond length are alternating,...long-short-long-short...that is, in the alternating system. With each delocalized orbital having only one electron, this band would be half-filled and might therefore be expected to be metallic[11] . However, the energy of the system is lowered if the  $\pi$ -electron density is increased between every alternate pair of carbon atoms to form a  $\Pi$ -bond in addition to  $\sigma$ -bond, i.e., if conjugated bonds are formed as shown in fig.2.5. An energy gap then appears in the middle of the  $\Pi$ -electron band between filled bonding states ( the  $\Pi$ -band ) and empty anti-bonding states ( the  $\Pi^*$ -band ), lowering the energy of the filled states. For polyacetylene this bandgap is approximately 1.7eV, so pristine polyacetylene shows not metallic conductivity but only a very small semiconductor like-conductivity.

The extra  $\Pi$ -bond causes the pair of atoms with the double bond to move slightly closer together. This dimerization and the associated bandgap reflect that a  $1 - D$  metal is unstable in the presence of interactions such as the electron lattice coupling(the Peierls instabilty ). In fact, abintio calculations indicate that the dominant

cause of the dimerization in polyacetylene is electron-electron interactions[9] , particularly atomic correlation. Since dimerization ( distortion ) can start from whichever ends of the chain trans-PA has two configuration having the same ground states. The existence of such degenerate ground states will help us in studying elementary excitations. The presence of conjugated bonds indicates the presence of relatively weakly bound  $\pi$ -electrons, with the possibility of metallic behavior if there exists a mechanism to eliminate the band gap between the filled and empty states. As Chiang et al (1977) showed, this can be achieved by doping with an electron acceptor such as iodine, as a result of which additional states are formed in the  $\Pi - \Pi^*$  band gap: electrons are transferred from the polymer chain to the dopant, and the mobile charged excitations become possible.

# Chapter 3

## Quasi-particles

The modern band theory of condensed matter is based on the assumption of the existence of a stable low-lying ground state and excited states above it. In most cases the energy of an excited state ( with respect to the ground state ) can be expressed as a sum of the excitation energies of elementary particles or quasi-particles ( such as solitons, polarons and bipolarons ). Hence, the electronic properties of conducting polymers would be governed by these non classical charge carriers: namely, the non-linear excitations ( quasi-particles ).

### Solitons

Currently, the term soliton is applicable in a wide area of physics such as particle physics, condensed matter etc. It also often used in the discussion of the existence of solitons and anti-solitons in polyacetylene. Forinstance, consider two ground state of trans-polyacetylene, say phase A and B, respectively. Both phases have exactly the same energy, and are idealized, in the sense that no kinks ( misfits ) or domain walls appeared ( see fig.3.1(a)&(b)). Suppose now the two undimerized PA (polyacetylene) under goes dimerization, i.e disorder to order (Peierls) transition. Assume

that dimerization starts simultaneously at both ends of the polymer chains and propagate to the center. When they meet, there is 50 % probability of misfit ( two single bond meet ) see fig.3.1. This misfit or domain walls separates the polymer chain into phase A and B, which are termed a "domains". In chemical language, there is a non-bonding orbital, in the neutral, uncharged ( i.e. undoped ) chain is occupied by a single electron that we can think as given by  $2p_z$  orbital of the C-atom with out double bond. These domain walls are conjugation defects ( bond alternating defects ) and their corresponding excitations is solitons. This excitations of the chain is spin  $\frac{1}{2}$  and charge 0 state. In other words, a free radical.

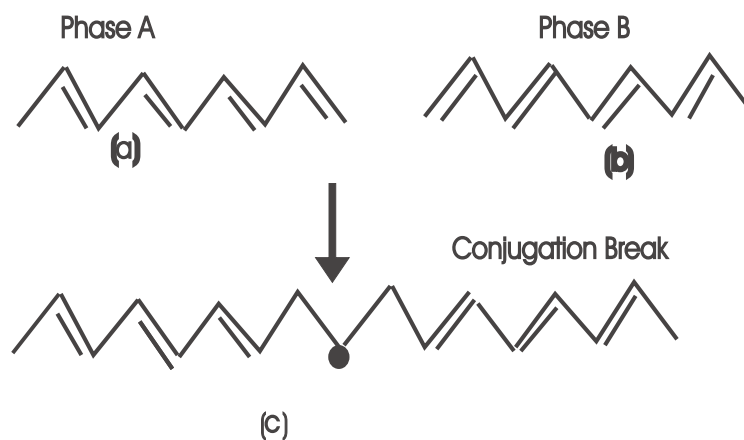


Figure 3.1: (a) and (b) stands for ground state degeneracy of two phases of dimerised trans-PA (c) a domain wall(soliton) separating the two phases of trans-PA chain

We recall that the cause of energy gap in conducting polymer is un interrupted double and single bond alternation. However, at the misfit ( soliton site ) the bond alternation is interrupted, and therefore there is no gap. At the misfits the atomic orbitals do not "know" whether they form non bonding ( $\Pi$ ) or anti-bonding( $\Pi^*$ ) states, Thus they form non-bonding states in the energy gap, and because of symmetry reasons

they form a mid-gap state. Apart from the structural distortion during synthesis (

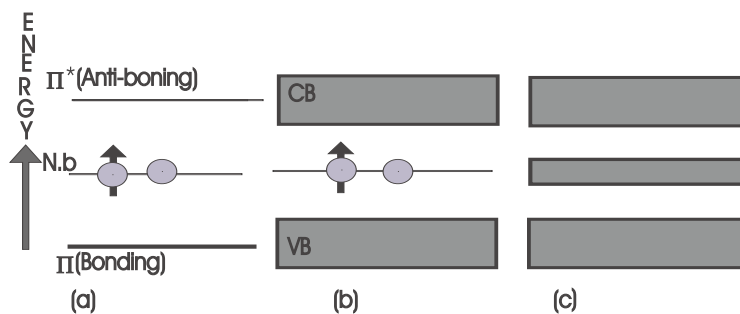


Figure 3.2: (a)Formation of mid gap-state due to the creation of soliton. (b)The anti-bonding form from the CB and the VB of the intrinsic conducting polymers (c)The soliton band

dimerization ) that resulted the creation of soloitons: doping is also another mechanism that changes the structure the structure of polymers and forms a mid gap state. Several works revealed that doping induces solitonic, polaronic, or bipolaronic states in the energy gap.

Physically, the soliton is represented as a transition region between two regions with alternating double and single bonds. With in the transition region the bond length is between the carbon atoms are almost the same ( see fig 3.1(c) ) in contrast to the dimerised double and single bond regions around the transition region. The new energy state ( mid-gap ) state can accommodate up to two electrons. If one electron alone occupies this level, the soliton is neutral and carries a spin. The other two possible states are charges states with zero and two electrons respectively, but with out any net spin. New optical transition are thus associated with these types of solitons and are consequently observed in optical spectra. The three cases are shown in fig 3.3. and small thick arrows indicate electron spin, dashed vertical arrows indicate

possible absorption transitions.

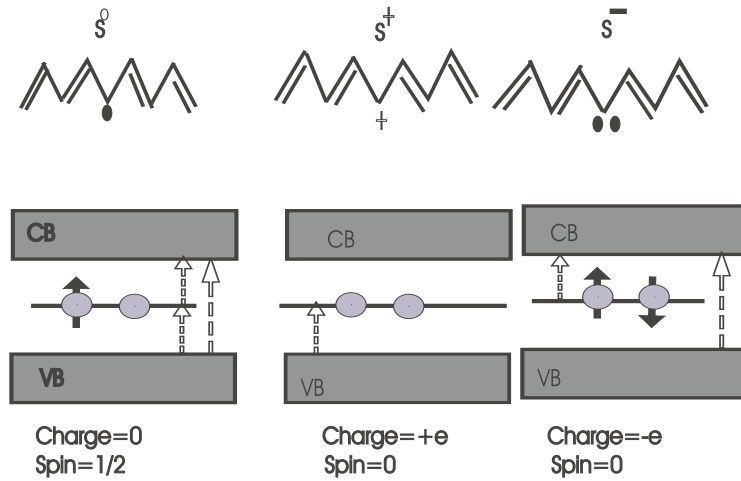


Figure 3.3: Solitons and electronic states, their charge, spin state, and their corresponding electronic transition

From the above discussion, the soliton species presents an "inverse" spin charge relationship i.e, when a charge is present there is no spin, and vice versa. It is also "inverse" as compared to the effects in conventional semiconductors.

Hence, solitons are localized over a certain distance, but mobile excitations. Generally, soliton formation results in the creation of new localized electronic states that appears in the middle of energy gap. However, at high doping levels, the charged solitons interact with each other to form a soliton band, which eventually merge with the band edges to create true metallic conductivity.

## polarons and bipolarons

Most conjugated polymers, including cis-polyacetylene, have non-degenerate ground states i.e polymers with two different ground states, having the aromatic form and quinoidal form ( see fig 3.4 ). These two forms differ in the position of the double bond. The aromatic form is energetically the more stable. Hence the left and right sides

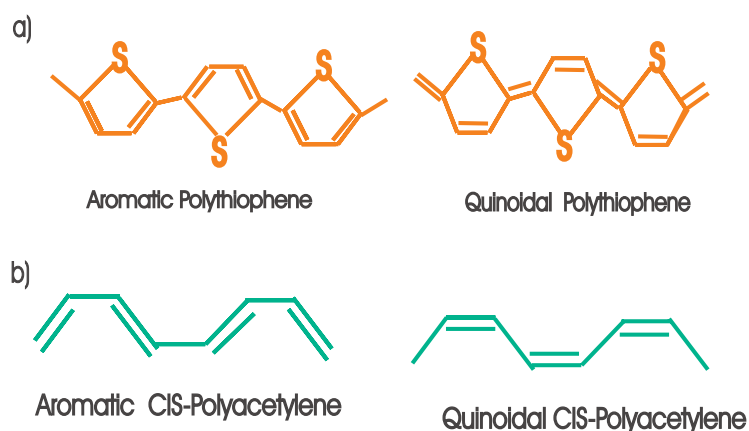


Figure 3.4: The aromatic and Quinoidal form of (a) polythiophene and (b) Cis-polyacetylene

of the misfit in polythiophene shown in fig 3.5. have different energies. This energy difference makes the misfit or the soliton energetically unstable. Consequently, the soliton moves in the direction shown in fig 3.5 and changes the high energy quinoidal rings in to low energy aromatic rings. Therefore, solitons in non-degenerate polymers are energetically unstable. To create a stable defects in non-degenerate polymers, we should have double-bound defects called polarons. Here one of the defects must be neutral while the other is charged negatively or positively. If the other is negatively charged it will be a electron polaron whereas if it is positively charged it will be a

hole polaron. These charge carriers are generally formed from charge transfer. If the dopant is an electron acceptor, charge transfer takes place from polymer acceptor, whereas if it is a donor, charge will transfer from dopant to polymer. Here an acceptor and donor counter ions reside between polymer chains.

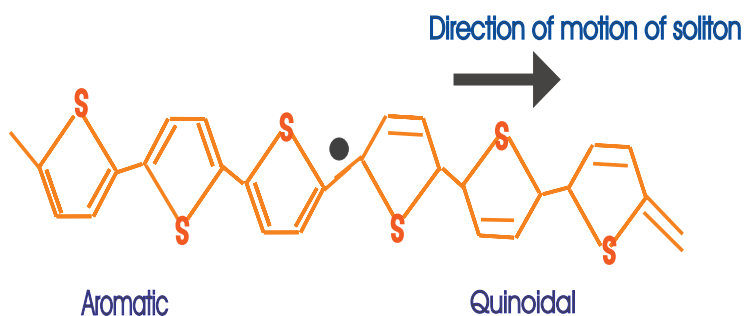


Figure 3.5: Unstability of soliton in non-degenerate polythiophene.

If two polarons exist in one chain, they will move towards each other to minimize the energy and form bipolarons. Here the neutral defects interact and form a bond while the charged solitons remain at a minimum separation of four rings. So bipolarons are doubly charged spinless charge carriers. Contrary to polarons that form "instantaneously" upon injection or photogeneration a charge, bipolarons are not created directly but must form by coupling of preexisting polarons, or possibly by the addition of a charge to a preexisting polaron as shown in fig.3.6. That means, energy of the two polarons is greater than the energy of a bipolaron ( $E_b < E_p$ , where  $E_b$  and  $E_p$  are energy of bipolaron and polaron respectively). That is electron-electron coulomb correlations are relatively weak compared to the energy difference between a bipolarons and a pair of isolated polarons. There is a considerable possibility that an electron and hole polarons interact to to yield a bound electron-hole pair called

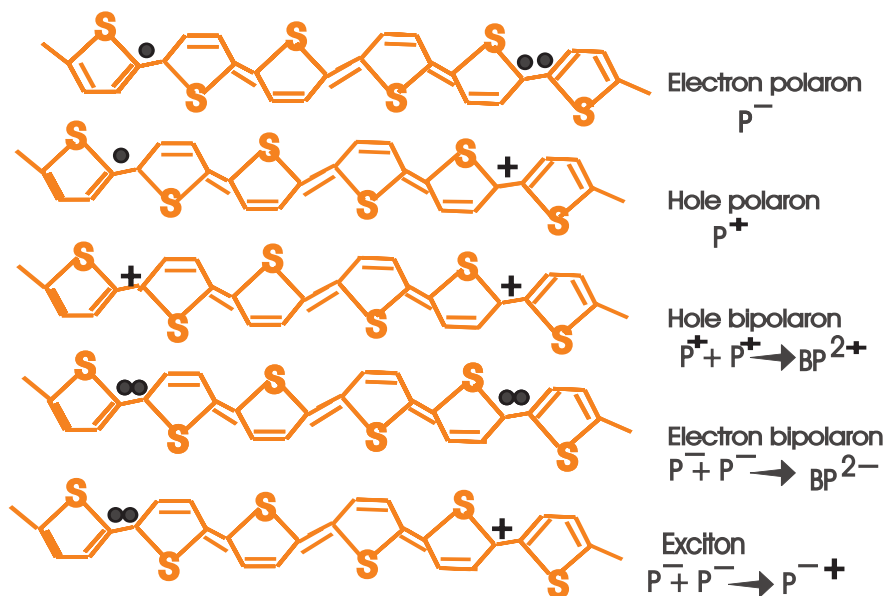


Figure 3.6: The four possible states of polythiophene

an exciton. ( see fig.3.6 ).

Excitons can be produced by the photo-injection. That is, an incident photon is absorbed by an electron in the valence band and jumps to the conduction band leaving a hole in the valence band. These electrons-hole pairs in polymers created as a result of photon absorption are bound together. This mechanism is photo-generation of charge carriers [6,13]. Polarons and bipolarons defects gives rise to the formation of two interacting states in the band gap. These two states are symmetric with respect to the gap center. The presence of new electronic states in the band gap makes new electronic transitions possible as shown in fig.3.7.

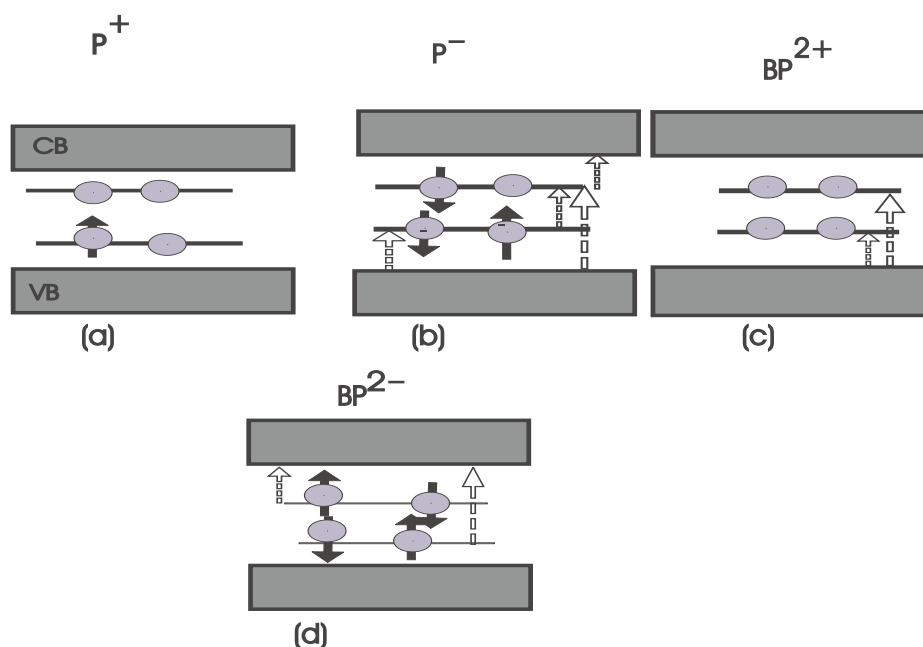


Figure 3.7: Energy band diagram for (a) hole polaron, (b) electron polaron (c) hole bipolaron (d) electron bipolaron

### 3.1 Doping in conducting polymers

Doping is the addition of "impurities" (dopant) to the bulk material, in order to alter the electrical properties of it. The role of the dopant is either to add holes to (i.e., remove electrons from), or to add electrons to the material. The former process is called p-doping and the latter n-doping. Doping is a concept of great importance in electroactive molecular materials and polymers. For instance, when Shirakawa et al., treated their polyacetylene film with elemental halogens, the conductivity was increased by the factor of over ten million. The P-doped polyacetylene they found a conductivity comparable to ordinary metals (see fig.3.8).

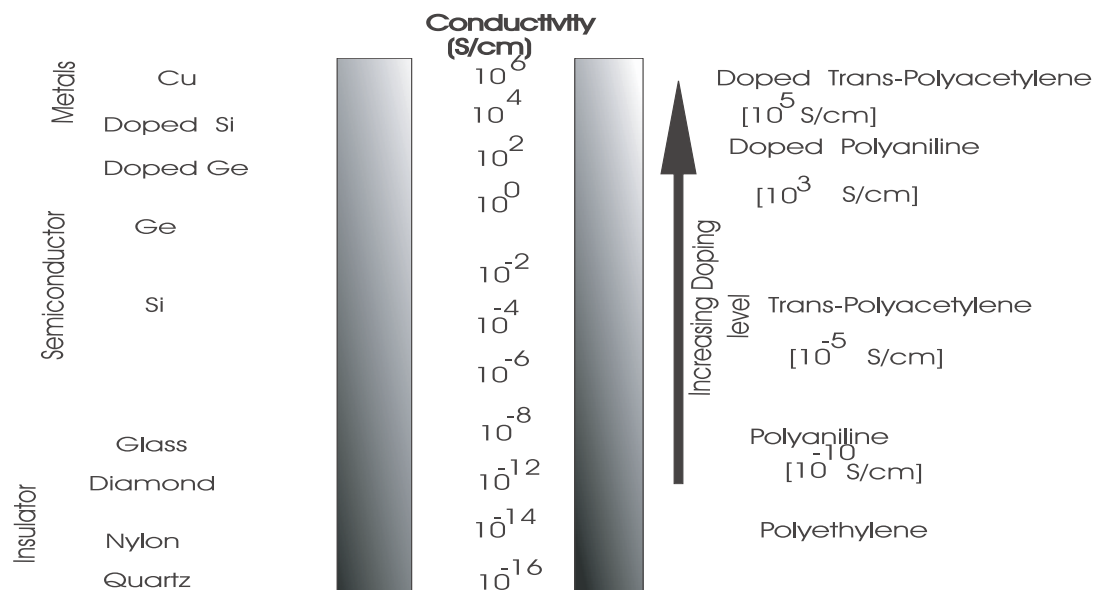


Figure 3.8: Conductivity of few Organic and Inorganic Materials Adapted from ref.16.

As can be seen in fig.3.9, the doping of polyacetylene with iodine creates a cation-radical on the polymer backbone ( i.e., oxidation ). This is referred to as a polaron. The moving of the polaron along the polymer chains equals the electrical current flowing through the material. Because of coulombic attractions between the polaron and the counter ion, which has a very low mobility within the material, the polaron is rather localized. This explains why so much dopant ( high concentration of counter ion) is needed in order to achieve metallic conductivity in these polymers. Inorganic semiconductors, as a comparison, often contain less ppm of dopant[14]. In other words, in inorganic semiconductors doping occurs via the introduction of dopant atoms that provide additional free charge carriers at room temperature so that the extra charges increase the conductivity for this type of charge carrier. As it is



Figure 3.9: Doping of Polyacetylene gives polaron

known, the Fermi level would be moved towards the CB ( conduction band ) if extra electrons are introduced or towards the VB ( valence band ) if the concentration of mobile holes has been increased. In organic semiconductors " doping " is usually achieved by the introduction of foreign molecules rather than atoms which can cause the local geometry modification of the chain that affects the electronic structure by introducing electronic states in the energy gap. In general the mechanisms by which high conductivity is achieved in polymers are quite different from those in doped semiconductors. The impurity atoms or molecules do not substitute for atoms of the polymer chain but are incorporated interstitially, i.e, they take up the locations between the chains, which leads to the production of radical cations or anions on the polymer chains each associated with an inert counter ion. Moreover, changes of the concentration of mobile charges are often achieved by trapping of e.g electrons in the CB sothat the concentration of mobile holes in the VB ( relative to the mobile of electrons ) increases. That way the Fermi level would move towards the VB and make the material a " doped " P-type material ( conductor ) i.e, a better hole than electron transport material. Since there is no net increase of mobile charge carriers the conductivity can not increase ( unless the mobility of charge carriers is affected

). A different form of doping resulting in a truly increased concentration of mobile charge carriers on the semiconducting molecule and therefore considerably increased conductivity can be achieved by complexation with foreign molecules. Such doping molecules are preferably large ( polymers ) so that they can not diffuse and penetrate into another material ( e.g, in pn-junction device ) where they can possibly neutralize with another (different) dopant to form a salt. Examples are doping of PANI with camphor-sulfonic acid or PEDOT with polystyrene sulphonic acid[15].

### **3.2 charge transport and conductivity in conjugated polymers**

As we know, the bandgap of insulators is so large as ( over 3-4eV ) for any excitation of charge of carriers to occur. The reason for this wide badgap in insulators is that the valence band is made up of bonding orbitals, which are completely filled, while the conduction band is constructed of anti-bonding orbitals of much higher energy. If a charge is injected in to an insulator, it has no energetically favorable way to travel with in the material. Electric current is, by definition, the uniform motion of charges, For this reason, the insulating material does not conduct electricity. Inorganic semiconductors have a narrow band gap ( under 3eV ), which allows some excitation of charge carriers to the conduction band. Since the overlap between the two bands is not very efficient, semiconductors usually have conductivities much lower than true metallic conductors. When the temperature is lowered, the probability of thermal excitation to the conduction band is diminished, which explains why conductivity of semiconductors decrease with decreasing temperature. Anisotropy is very common among semiconductors. Inorganic semiconductors often have relatively high mobility

$\mu$ , but their conductivities are limited by the number of charge carriers  $n$ . Metallic conductors, have either an incomplete valence band, which is the case for all transition metals with their unoccupied d-orbitals, or a near zero bandgap between the valence band and the conduction band. Both these situations lead to a continuous and partially filled band. Metallic conductors have a very large number of charge carriers  $n$  (" free electrons "), but are instead limited by a relatively low mobility  $\mu$ . Thermal excitation leads to scattering of charges, which makes it less probable for them to move ideally along the current axis, hence lowering the conductivity. This explains why conductivity decreases with increasing temperatures in metallic conductors[6]. Still, the conductivity in metals is much greater than in inorganic semiconductors. Conducting polymers behave more like, amorphous semiconductors, is due to low coupling ( interaction ) between the molecules, the carriers in these materials are strongly localized in a molecule. Transport occurs via a sequence of charge transfer steps from one molecule to another, similar to the hopping between defect states in organic semiconductors that means the electrons are not moving in bands but are localized at a specific states in the gap. They hop between these localized states. The charge transport process of a conjugated polymer can not be explained by one single model over the whole conductivity ranges, from insulating to metallic. Different models must be applied for different polymers in various regions. The different conductivity regions are due to different levels of doping. For undoped or lightly doped conjugated polymers, the electronic properties show a behavior, with zero ( or low conductivity ) at  $0^{\circ}K$ . This Low( zero ) conductivity leads to the conclusion that the concentration of mobile free charge carriers is low. The charge transport is then

explained by hopping between localized solitonic, polaronic or bipolaronic states according to Mott's variable range hopping (VRH) model [17]. This Model assumes that the localization of the states is weak, allowing electrons to jump further away than to the nearest available site, there by making it possible for them to find a state with lowering energy than the nearest neighbor state. The term variable range describes this flexibility in finding an appropriate site. When the temperature increases, the number of available states rises and the average hopping distance decrease, resulting in a higher conductivity. The temperature dependence of the electrical conductivity is described by

$$\sigma = \sigma_o(T)exp[-(\frac{T_o}{T})]^\gamma \quad (3.2.1)$$

where,  $\gamma = \frac{1}{1+d}$ ,  $d$  is the dimensionality of the system,  $d=1,2,3$   $\sigma_o(T)$  varies more slowly than the exponential factor, and the characteristics temperature  $T_o$  is related to the density of states  $N(E_F)$  and the localization length 'a' as

$$T_o \sim \frac{1}{a^d N(E_F)} \quad (3.2.2)$$

Mott's  $T^{-\frac{1}{4}}$  law has a limitation since it is strictly following one dimensional nature of solitons ( no interchain hopping), to circumvent this difficulty Kevelson, proposed an intersoliton hopping model[18]. According to this model, motion of a simple soliton at the discontinuity along the polymer chain does not lead to charge transport, but an inter chain soliton hopping mechanism could contribute to conduction with conductivity varying as a power of temperature. However, the agreement of a vast amount of conducting polymers data with a hopping laws over a wide temperature

range suggest that once localized states are formed in the gap by whatever mechanism, conduction takes place predominantly by the usual VRH process for lightly (undoped) doped polymers.

In heavily doped samples, as mentioned before, the overlap of wave functions that a metallic picture is like to be more appropriate, at least in the ordered regions. Hence, a model with small conducting islands with metallic conductivity is separated by insulating barriers is used. These barriers could be different kinds of inhomogeneities like conjugational defects or undoped chains segments. Charge transport through the material will then be limited by the fact charge carriers have to tunnel through these barriers. The most successful theories so far describing this type of conductivity have been presented by Sheng [17]. The model gives the temperature dependence of the conductivity given by

$$\sigma(T) = \sigma_o \exp\left[-\left(\frac{T_1}{T_o + T}\right)\right] \quad (3.2.3)$$

where the constants  $T_o$  and  $T_1$  are determined by the shape and size of the insulating barriers.

## Chapter 4

# Metal-semiconductor contact (Metal-CP contact)

An important aspect of any device is the property of contact between the electrodes and the active layer, which are responsible for charge injection. The choice of contacts in polymer based devices is an area of critical importance, as they can affect minority and majority current flow, and hence recombination rates and efficiency of the device. In inorganic semiconductors, such as Si, GaAs, the Schottky energy barrier formed at a metal contact depends weakly on the choice of metal. At the metal-semiconductor interface of an organic semiconductor; there is a much wider variation in the values of the observed barrier height. In fact, the operation of polymeric devices depends on the asymmetry of the barrier heights at the two contacts. ITO is the preferred anode material due to its transparency and relatively high work function. On the other hand, metals, such as Al, Ca, and Mg with lower work functions are employed as cathode materials. Although metal semiconductor contacts are often referred to as schottky contacts in literature, this is not always the case, and they can be of one of the following: low resistance of ohmic contacts, or rectifying contacts.

Fig.4.1.illustrates the formation of a metal-semiconductor Schottky contact(the formation of an ohmic contact is discussed below). Although this discussion is based upon inorganic semiconductor theory, it is applicable since we are dealing with band models. As the metal is brought in to contact with the n-type semiconductor, thermal equilibrium is established and the Fermi levels in the metal and the semiconductor become continuous and equal through both materials. In order for the Fermi-levels

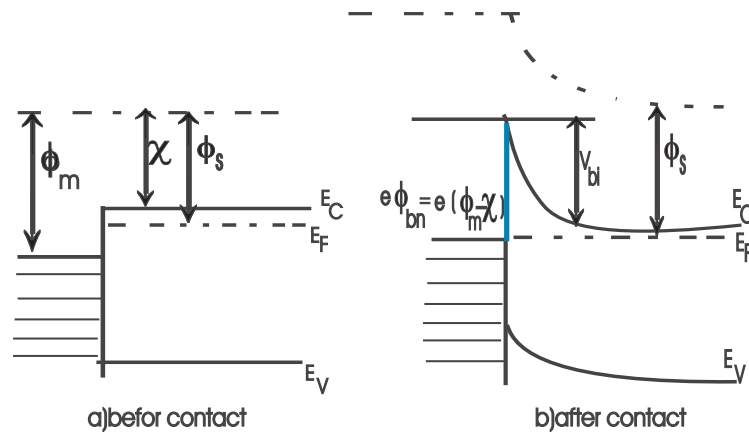


Figure 4.1: The energy band diagram of (a)an isolated metal adjacent to an isolated n-type semiconductor under non equilibrium condition (b)a metal-semiconductor contact in thermal equilibrium

to align, electrons from the semiconductor should flow in to the metal, leaving behind positive ionized donors in the semiconductor. Therefore, the bands bend as shown in fig.4.1 and a Schottky diode is formed, provided that  $\phi_m$  exceeds the semiconductor work function,  $\phi_s$ . If the semiconductor is p-type, electrons are injected from the metal into the semiconductor, causing a build up of negative charge in the semiconductor, and consequently the bands bend the other way if  $\phi_m < \phi_s$  see fig.4.2. Organic semiconductors have negligible doping and no intrinsic carriers due to the

wide band gap, so no band bending occurs ( as compared to inorganic semiconductors). The barrier heights to electron and hole injection,  $\phi_{Bn}$  and  $\phi_{Bp}$  respectively, can be calculated as follows:

$$e\phi_{bn} = e(\phi_m - \chi) \quad e\phi_{bp} = E_g - e\phi_{Bn} \quad (4.0.1)$$

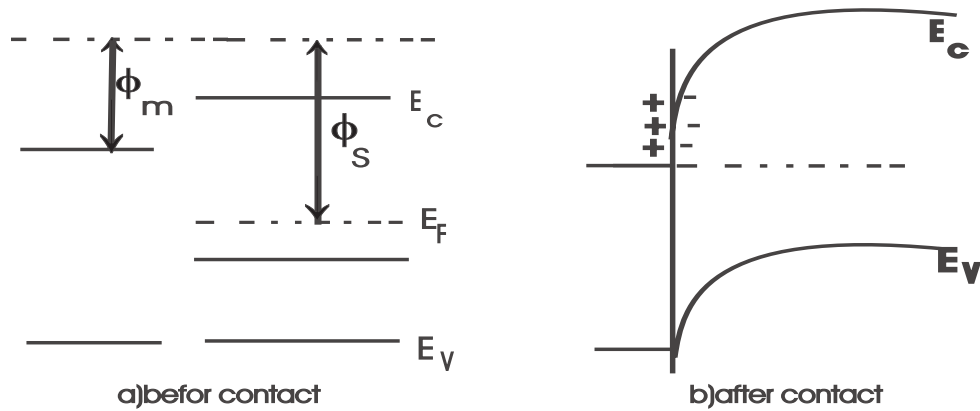


Figure 4.2: The energy band diagram of (a) an isolated metal adjacent to an isolated p-type semiconductor contact under non equilibrium condition (b) metal/p-type semiconductor contact under open circuit condition

An ohmic contact can also be formed at a metal-semiconductor junction by one of two methods. Firstly, a metal with a work function which is smaller than that of the semiconductor for n-type semiconductor ( $\phi_m < \phi_s$ ) or greater than that of the semiconductor for p-type semiconductor ( $\phi_m > \phi_s$ ), can be chosen and no barrier to carrier injection from the metal will be formed. However, this approach is not usually followed because the barrier height may be pinned by the high interface state density at the contact. A more practical approach of creating an ohmic contact is to form a Schottky barrier contact, with heavily doped semiconductor at the interface,

causing a narrow depletion width, significant band bending, and a barrier which is thin enough to tunnel through it [8,20,21].

For most organic semiconductors, increasing the free charge carrier density through the addition of dopants is difficult to achieve, and so an ohmic contact can not be achieved in this way. It is also difficult to make an ohmic contact via the choice of work function, particularly finding the values above typical HOMO levels or below LUMO levels[22,23]. In practice the barrier height is minimized by choosing appropriate contact materials.

## 4.1 Current-voltage Characteristics

Fig.4.3. Shows the conduction band profiles for a metal contact on an n-type semiconductor material in forward and reverse biases. Considering electron flow from the semiconductor to the metal, the potential barrier is reduced and the current  $J_{ms}$  (current flow from metal semiconductor) is increased. However, for electron flow from the metal to the semiconductor, the potential barrier to electrons is independent of the field if image forces are neglected. Therefore, the current for electron flow in this direction  $J_{sm}$  is a fixed contribution to the current flow in the forward bias, which is matched by  $J_{ms}$  at thermal equilibrium. Under reverse bias conditions, the potential barrier to electrons flowing from the semiconductor to the metal increases, as does the depletion width, and so the current flowing from the metal to the semiconductor  $J_{ms}$  is the dominant component. This situation causes a highly asymmetric current-voltage characteristics similar to that of a pn-junction diode. However, current flow in a Schottky diodes is dominated by majority carriers, while in pn junction diodes it is dominated by minority carriers[21].

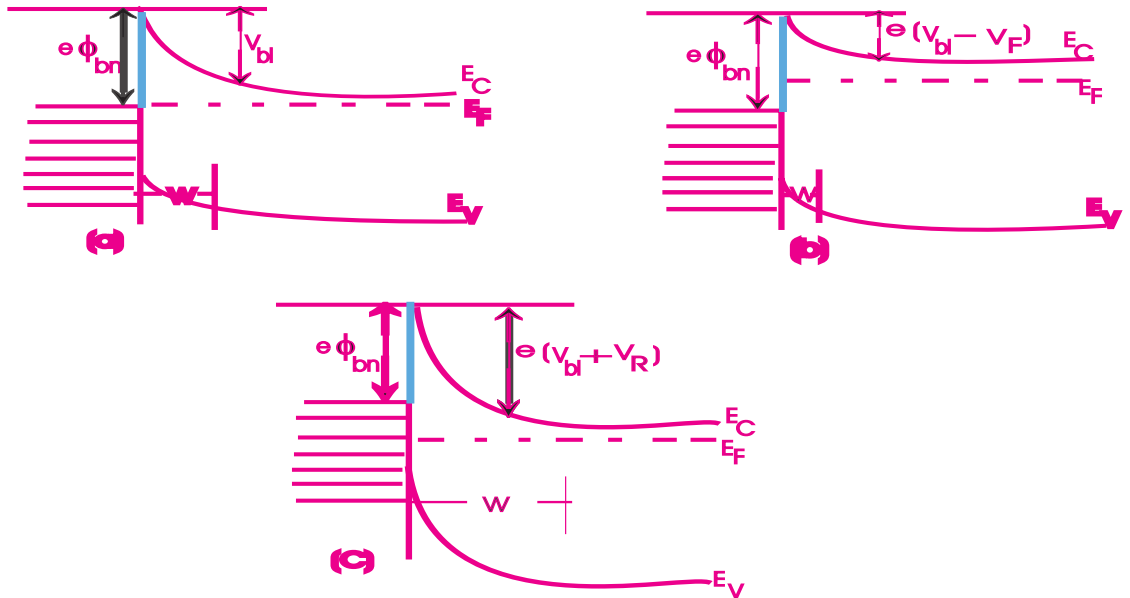


Figure 4.3: Energy band diagram of rectifying metal -n-type semiconductor contact at a) thermal equilibrium b) forward bias and c) reverse bias

Charge transport across the metal-semiconductor interface can be summarized as arising from the following three process:

- Transport of carriers from the semiconductor over the potential barrier in to the metal. This is the dominant process for moderately doped semiconductors.
- Field emission of carriers through the barrier.
- Recombination in the semiconductor, this corresponds to minority carrier injection.

Neglecting the other mechanisms and considering the dominant thermionic emission

related current, the current density-voltage characteristics of the Schottky diode is

$$J = J_o \left[ \exp\left(\frac{qV}{nkT}\right) - 1 \right] \quad (4.1.1)$$

Where  $J$  is the total current density (under dark),  $J_o$  is the reverse saturation current density flowing under sufficiently high reverse bias,  $q$  is the charge on an electron,  $V$  is the applied voltage,  $n$  is the ideality factor of the diode. (for an ideal diode,  $n = 1$ ),  $k$  is the Boltzmann constant, and  $T$  is the absolute temperature. The reverse saturation current density  $J_o$  is given by

$$J_o = A^* T^2 \exp\left(\frac{-q\phi_B}{kT}\right) \quad (4.1.2)$$

Where  $A^*$  is modified Richardson constant which express the number of electron at the semiconductor-metal contact that may be injected into the metal and it also takes into account the effective density of states in the conduction band. For organic semiconductor Schottky diode the modified Richardson constant is assumed to be that of free electron, which is equal to  $A^* = 120 A/cm^2 K$ .

There will be a different J-V characteristics which can be studied under three different situations depending on the relative magnitude of  $J_o$ . These are:

- i) If  $J \gg J_o$ , the contact will effectively block current flow for a reverse bias voltage and will display an exponentially increasing current for a forward bias. This results in a rectifying contact, which can be desirable for photovoltaic device.
- ii) If  $J \ll J_o$ , the junction readily passes current for both sign of the applied voltage.

In this case Eqn.4.1.1 can be expanded to yield

$$V \cong \left(\frac{nkT}{J_o q}\right) \quad (4.1.3)$$

this equation is linear in  $J$  and is Ohm's law.

iii) If  $J \cong J_o$ , i.e., If  $J$  and  $J_o$  are comparable, then the J-V curve is neither rectifying nor ohmic but symmetric. In the junction obeying the rectification, the condition i) we can find  $J_o$  by extrapolating the linear part of plot  $\ln J$ - $V$  to the  $\ln J$ -axis at small forward bias voltage. Determining  $J_o$  we can determine, the barrier height from the relation

$$\phi_B = \frac{kT}{q} \ln\left(\frac{A^*T^2}{J_o}\right) \quad (4.1.4)$$

and the ideality factor ( $n$ ) of the device can be obtained from the plot of  $\ln J$ - $V$ . The slope of  $\ln J$ - $V$  is given by

$$slope = \frac{\partial \ln J}{\partial V} \quad (4.1.5)$$

Then the ideality factor,  $n$  can be calculated easily from the relation

$$n = \frac{q}{kT\left(\frac{\partial \ln J}{\partial V}\right)} \quad (4.1.6)$$

or ideal diodes, the diode quality factor,  $n=1$ . All real diodes have  $n > 1$ , since trapping and recombination of charge carrier is high.

In an organic based device, the built in voltage is taken to be the difference between the two metal work functions (see fig 4.4).

Fig.4.4 shows a typical metal semiconductor contact which has ohmic in nature on high work function metal side (metal1) and rectifying contact with low work function metal (metal-2).

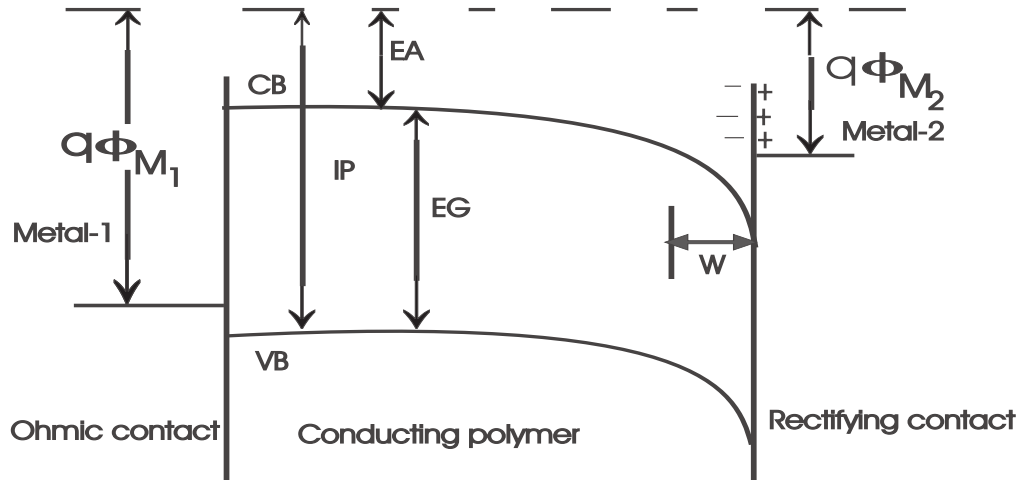


Figure 4.4: Energy band diagram of Metal/p-type conducting polymer/Metal Schottky barrier under open circuit condition

## 4.2 Impedance spectroscopy and Modelling concept

Impedance spectroscopy is a relatively new and powerful method of characterizing many of the electrical properties of materials and their interfaces with electronically conducting electrode. Using this one can find the resistance(  $R$  ) and capacitance(  $C$  ), of the junction formed by two electronically conducting materials. Impedance is measured in the frequency domain by applying voltage or current to the device under test ( DUT ) and measuring the resulting current or voltage. The impedance is expressed as a complex number,

$$Z = Z_r + jZ_i \quad (4.2.1)$$

where  $j=\sqrt{-1}$  and  $Z_r$  and  $Z_i$  are the real and the imaginary parts of the of the impedance respectively.

The real and imaginary components of the impedance are recorded as a function of frequency and plotted in complex plane. The real part,  $Z_r$ , is in the direction of real axis X, and the imaginary part,  $Z_i$ , is along the Y axis. Hence, an impedance of  $Z(\omega)=Z_r+jZ_i$  is such a vector quantity and may be plotted either in the rectangular or polar coordinate in fig.4.5. One of the most attractive feature of impedance

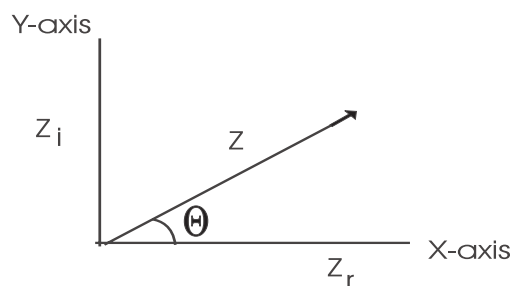


Figure 4.5: The impedance plotted as a planar vector using rectangular and polar coordinate.

spectroscopy lies in its applicability to studies the development of direct correlations between the response of a real system and an idealized model circuit composed of discrete electrical components [24,25] . For the interface formed by metal-polymer contact, the resistance( R ) represents the dissipative component and the capacitance( C ) describes the storage component. These resistances and capacitances can be combined in a variety of forms according to the interface formed and finally leading to an array of phenomenologically models.

We shall begin by modelling the junction between aluminium and polymer as a simple

parallel RC circuit as depicted in fig 4.6. The total impedance of this model is given by

$$Z = \frac{R}{1 + j\omega RC} \quad (4.2.2)$$

Rationalizing and rearranging terms results

$$Z = \frac{R}{1 + \omega^2 R^2 C^2} - \frac{jR^2 \omega C}{1 + R^2 \omega^2 C^2} \quad (4.2.3)$$

where  $Z_r = \frac{R}{1 + \omega^2 R^2 C^2}$  and  $-Z_i = \frac{R^2 \omega C}{1 + R^2 \omega^2 C^2}$

The Cole-Cole plot of this impedance  $-Z_i$  versus  $Z_r$  in its ideal form is depicted as in fig.4.6(b). Ideally the imaginary part of the impedance is zero at frequencies,

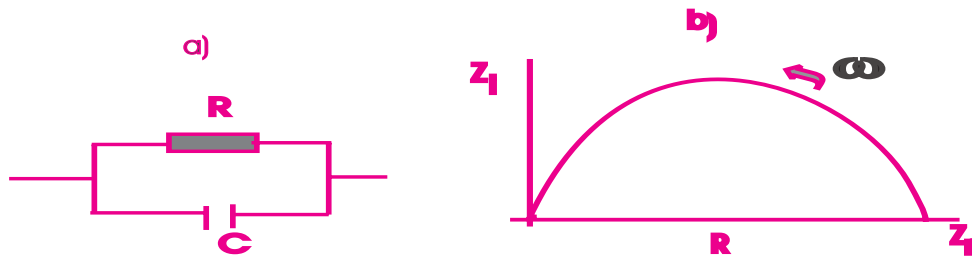


Figure 4.6: a)RC-parallel circuit b)Ideal Cole-Cole plot of the impedance of parallel RC circuit.

$\omega=0$  and  $\omega$  approach to  $\infty$ . This plot forms a semicircle with the center on the real axis. The diameter of the semicircle corresponds to R.

Taking the derivative of  $Z_i$  with respect to angular frequency, we get

$$\frac{dZ_i}{d\omega} = \frac{-CR^2(1 - \omega^2 R^2 C^2)}{1 + \omega^2 R^2 C^2} \quad (4.2.4)$$

Eqn.4.2.4 becomes zero when  $\omega = \frac{1}{RC}$

by combining Eqn.4.2.4 and the imaginary part of Eqn.4.2.3 we get

$$-Z_{imax} = \frac{R}{2} \quad (4.2.5)$$

Thus, using Eqn.4.2.5 we can calculate the unknown resistance directly from  $Z_{imax}$ .

If there is a contact resistance  $R_c$  in series with RC parallel circuit, the impedance of the circuit becomes

$$Z = R_c + \frac{R}{1 + j\omega RC} \quad (4.2.6)$$

and the Cole-Cole plot will be as in fig.4.7.

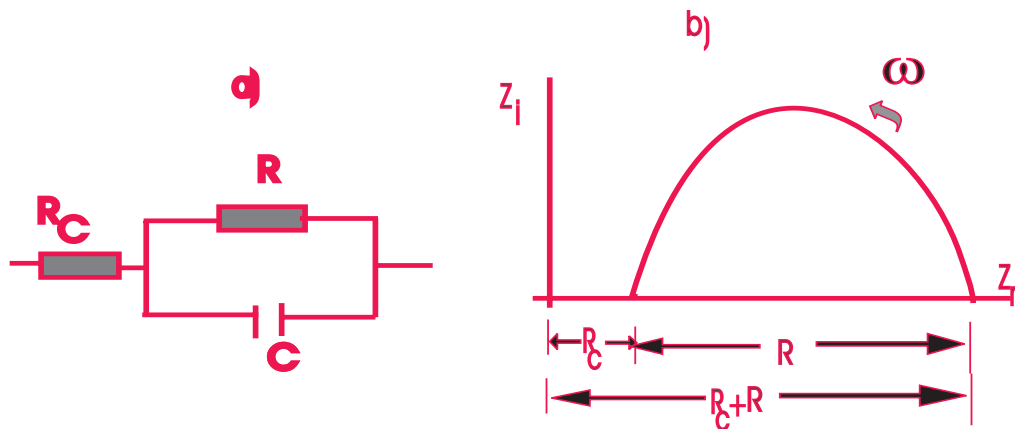


Figure 4.7: a) RC-parallel circuit connected in series with contact resistor b) Its Cole-Cole plot.

# Chapter 5

## Photovoltaic phenomena in conducting polymer devices

### 5.1 Review

Solar energy is the most important sources of renewable energy that can be utilized for betterment of mankind's. The conversion of solar light in to electric power requires the generation of both negative and positive charges as well as a driving force that can push these charges through an external electric circuit. When connected to the external electric circuit or any electrical devices, such as a radio or the computer screen, may then utilize the converted solar energy.

In the last couple of years, the development of solar cells based on the organic molecules and conjugated polymers has progressed rapidly. Today, three different types of cells using organic molecules are under intense research investigation[26].

These are:

- dye sensitized nanocrystalline  $TiO_2$  solar cells
- molecular organic solar cells and
- polymer solar cells

The highest efficiencies among these solar cells (  $\sim 11\%$  ) have been reported for the dye sensitized noncrystalline  $TiO_2$  solar cells, which are based on photo-electrochemical principles. Molecular organic solar cells use organic dyes. The active layers are cast by vacuum evaporation techniques. The organic dyes show high absorption coefficient a good match of the solar spectrum. but their efficiency are limited by the low exciton diffusion length and low charge mobility of the materials. Efficiencies of 1% were already achieved. Recently the use of doped pentacene, which shows much higher mobilities, pushed up the efficiencies up to 2% for thin films and for single crystalline devices. The third type of organic solar cells, the polymer solar cells, should be discussed in more details since they are the basis for this work. Pristine polymer solar cells, sandwiched between asymmetric contacts, show low efficiencies because the inefficient charge generation in the polymer layer. The discovery of photoinduced charge transfer from  $\Pi$ -conjugated polymer to fullerene opened a new way for solar cells and photodiodes. The efficiency for this process is near unity, i.e, this process is much faster than any competing radiative and non-radiative relaxation path ways. Bilayer devices from conjugated polymers and  $C_{60}$  fullerene shows improved efficiencies. But as for molecular cells, only the light absorbed with in the distance of the diffusion range of excitons to the heterojunctions contributes to the current.

A breakthrough for polymer solar cells was the introduction of the bulk heterojunction concept, which consists of an interpenetrating network of a conjugated polymer and fullerene. It leads to efficient and fast charge generation with in the whole bulk. Different research reports indicated that improving the electrical contact

interfaces and morphology have been to be crucial parameters for device efficiency. In this research, the bulk heterojunction photovoltaic devices based on poly[3-(2,5-dioctylphenyle) thiophene] (PDOPT) as donor, which is a band gap of about 2.02eV, together with a soluble fullerene derivative (PCBM) as acceptor with a PEDOT:PSS, hole transporting layer were fabricated. Photovoltaic performance parameters were characterized.

## 5.2 Photogeneration of free charge carriers

Most conjugated polymers have semiconductor band gap of 1.5-3eV, which means they are ideal for optoelectronic devices that work in the visible range of the electromagnetic radiation spectrum. This property of the conjugated polymers prompted research in the area of photovoltaic devices where conjugated polymers used as the active layer. Photovoltaic cells based on inorganic semiconductors such as silicon that absorb light at energies above the band gap, can excite electrons over the band gap from valence band to the conduction band, leading to the automatic separation of positive and negative charge carriers. These charge carriers then migrate separately through the semiconductor material and collected under the internal electric field to opposite electrodes, giving rise to an open circuit voltage or with an external load, a photocurrent. Unfortunately this is not the case in conducting polymers since the excitons formed by absorption are bound by Coulomb interaction between electron in the LUMO and hole in the HOMO are very strong and are not readily dissociated i.e, the exciton binding energy exceeding  $kT$  by more than an orders of magnitude. Thus, to generate free charge carriers, the excitons must be dissociated. This can happen

in the presence of high electric field, at the defect site in the material, or usually, at the interface between two materials that have a sufficient mismatch in their energy levels[27,28]. Thus, an organic solar cell can be made with different layered structures, some of them will be discussed in details.

### 5.2.1 Schottky Junction(Single layer)devices

This is the simplest interface created at the junction between the electrode and the conjugated polymer. The structure of the Schottky solar cells used the configuration ITO/polymer/Aluminium. Under open circuit conditions, holes are collected at the high work function electrode (ITO), and electrons are collected at the low work function electrode ( aluminium ). Indeed, the open circuit voltage,  $V_{oc}$  generated by these devices depends upon the work function difference between the two electrodes ( see fig.5.1 ). In such interfaces, the excitons formed by absorption of photons in conjugated polymers ( CPs ) are only split in to separate charge carriers when they encounters an interface between materials of different electron affinity, such as that between a CP and aluminium followed by the dissociation of the the exciton at the interface and migration of the separated charge carriers to opposite electrodes.

An easy and good model to describe a polymer diode is the metal-insulator-metal diode ( MIM ), introduced by Parker for light emitting diodes[26,29,30].The polymer assumed to have a negligible amount of intrinsic charge carriers and can therefore be seen as insulator.

Fig. 5.1 shows a pristine polymer devise under different working conditions within MIM picture.Fig.5.1(a) shows short circuit case, where photo created holes are transported to the ITO contact electrons the Al. The driving force for the separation is the electric field across the polymer layer. The electric field is constant over the whole

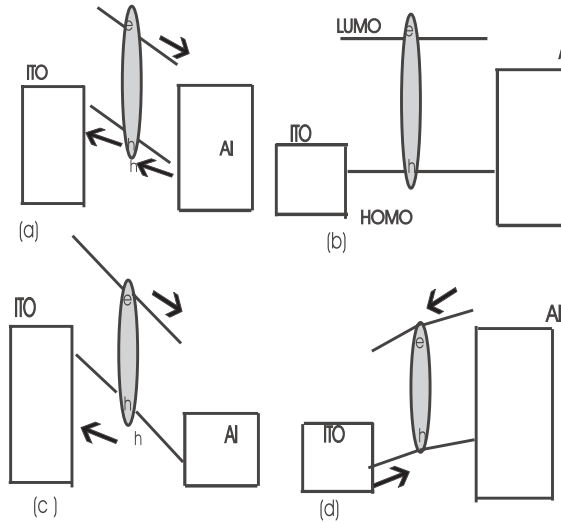


Figure 5.1: MIM picture for polymer diode under different working conditions (a) Short circuit, under illumination photogenerated charges drift to ward the contacts. (b) Flat band or open circuit under illumination, the  $V_{oc}$  is the work function difference between the two contacts, (c) Diode under reverse bias, diode work as photodetector, and (d) Diode under forward bias, diode can work as light emitting diode.

layer and is provided by work function difference of the contacts. Under open circuit conditions and illumination, this case is shown in fig.5.1(b), the created charges show no preferred direction. The open circuit voltage cancels the potential difference of the contacts. The maximal observed open circuit voltage,  $V_{oc}$  should be the work function difference between the two contacts. In the case of ITO and Al it should be 0.4V. In the case of a negative applied bias, i.e. positive contact to the Al and negative to the ITO, the diode works as photodetector[29]. It is presented in fig 5.1(c). Photoinduced charges are selectively transported, assisted by the external field, to the contacts, holes to ITO and electrons to the Al. Under forward bias, electrons are injected from the

Al to the conduction band and holes from the ITO to the valence band. The observed net current is dominated by the recombination of the two charge carriers. If electrons and holes recombine radiatively, electroluminescence can be observed[29]. The MIM picture explains well the diode behavior of the devices as well as the solar cell activity of single layer devices. However, in bulk heterojunction devices the observed  $V_{oc}$  of MDMO-PPV/PCBM device  $> 0.8V$  is not in accordance with the work function difference of ITO and Al of  $0.4V$ .

Under illumination, the current flows in the opposite direction than the injected currents. As in fig.5.1(a) the maximum generated photocurrent flows under short circuit conditions (see also I-V curve in fig.5.4 ); At (b) the photogenerated current is balanced to zero (flat band condition ). Between (a) and (b), as in the forth quadrant of I-V( fig,5.4 ), the device generates power( i.e  $I \times V$ ).

Generally, the J-V characteristics of an ideal photovoltaic device can be described by

$$J = J_{ph} - J_d \quad (5.2.1)$$

where  $J$  is the net current density,  $J_{ph}$  is photogenerated current,  $J_d$  is the dark current density can be described as

$$J = J_{ph} - J_o[\exp(\frac{qV}{nkT}) - 1] \quad (5.2.2)$$

The need that carriers formed with in CPs find an interface at which to dissociate is one of the reasons why the overall efficiency of the best CP-based photovoltaic cells is low compared to silicon-based photovoltaic cells. Another cause of the very low efficiencies of such devices is the effect of impurities, such as oxygen which act as traps to the migrating excitons. Thus, the the exciton-splitting process that occurs

at a CP-electrode interfaces is not very efficient[30].

### 5.2.2 Donor-Acceptor Bilayer Devices

An organic solar cell can be made with the following layered structure: Positive electrode/electron donor/electron acceptor/negative electrode. It is a more efficient way to generate free charge carriers. In such kind of devices the conjugated polymer is used as an electron donor and organic molecule  $C_{60}$  or PCBM as the electron acceptor. Although at the first glance, the concept may be reminiscent of the pn-junction in inorganic materials, the physical process are often very different. The photogenerated excitons diffuses towards the donor-acceptor interface and dissociates to free charge carriers. The mechanisms involved in this process is that the highly electronegative,  $C_{60}$  dissociates the exciton and accepts an electron an electron. Fig.5.2(a) shows that the the required transfer of charges can be realized at the interface between two materials if one material has a higher electron affinity ( EA ) whereas the other has a lower ionization potential ( IP ). The one with larger EA can accept an electron from the CB of the other and the material with lower IP can accept the hole from the VB of the contacting organic molecule  $C_{60}$ . We note that the offset of IP and EA needs to be large enough so that the resulting field (the potential gradient at the junction) can overcome the exciton binding energy inorder to break-up photo-generated excitons. Other wise energy transfer may occur but the excitons do not split into their constituent charges and recombine eventually at the D/A interface ( see fig.5.2 (b) ). The exciton diffusion length limits the performance of such a devices.

The exciton diffusion length in a conjugated polymer is  $\sim 10\text{nm}$ . So the thickness

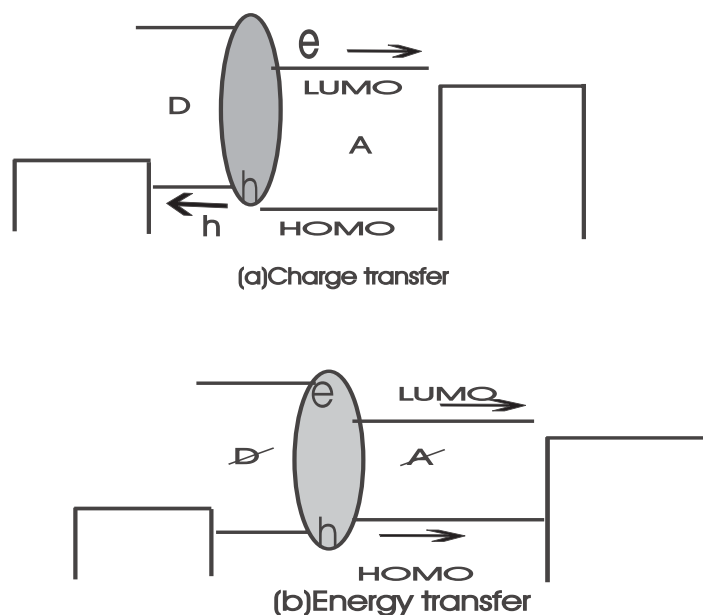


Figure 5.2: The interface between two different organic semiconductors can either: (a) facilitate charge transfer (D/A) interface (b) energy transfer forms depends on the position of HOMO and LUMO levels.

of such a devices should be small enough to make all the excitons reach the interface and have maximum efficiency. It is also to be noted that eventhough charge transfer process at the interface happens with in nano seconds, the transport property of  $C_{60}$  is poor, which results in low transfer of free charge carriers to the electrode, this increases the probability of recombination. Thus, this small diffusion range of the excitons compared to the film thickness necessary to absorb the major portion of light ( typically  $> 100\text{nm}$  ) made it light to reach practically interesting conversion efficiencies inorganic solar cells.

### 5.2.3 Bulk heterojunction solar cells

The most promising candidate of flexible plastic solar cells is used on the bulk heterojunctions structure, which consists of an interpenetrating network of conjugate polymer fullerene. Bulk heterojunction solar cells can be made by mixing the polymers with PCBM.

#### Basic principles

As it was indicated in the earlier sections, the efficiency of the free charge carrier generation as a prerequisite for a photovoltaic effect is typically very low in organic materials due to poor photoinduced charge separation and transport ( i.e, low mobility ) of photogenerated charge carriers. But, a successful method to the dissociation of excitons in organic semiconductors is at a so-called donor/acceptor heterojunction interface. This heterojunction work very well at separating excitons that arrive at the junction and enhances the probability of electron transfer between molecules. Unfortunately, the lifetime of excitons is short, and only excitons that are formed within  $\sim 10\text{nm}$  of the junction will ever reach it. This short exciton range clearly limits the efficiency of these devices. In an attempt to develop a more efficient photovoltaic structure, a nano-scale interpenetrating bicontinuous network of donor and acceptor polymers extending the interface area over whole photoactive layer device architecture often referred to as the bulk heterojunction. With these materials, the number of heterojunctions with the polymer blend is greatly increased ( i.e, the contact area between the n-and p-type polymer is maximized ) and thus the probability that an exciton will encounter a junction and be separated. Such a maximized interface area

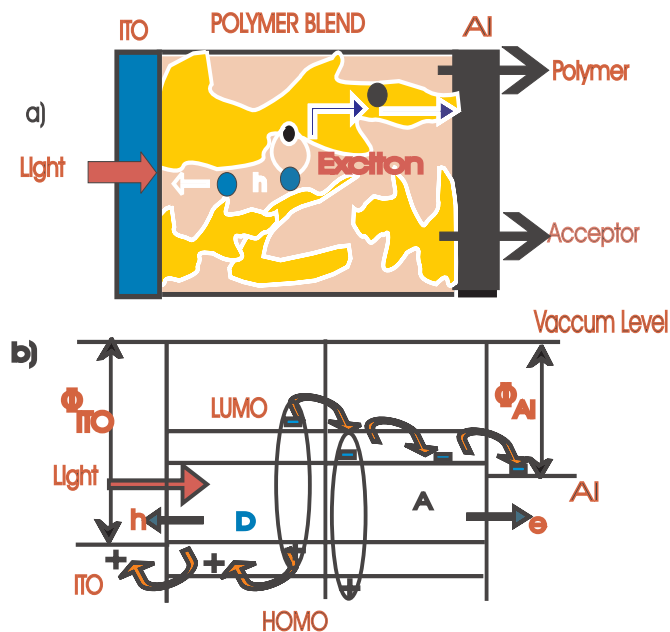


Figure 5.3: Schematic representation of a polymer thin film photoactive device, made of an electron-acceptor and a hole-transporting (HTL) polymer, with an arbitrary chosen mixing profile, an ITO anode and Al cathode: (TOP) and film cross section: (Bottom) energy diagram . Adapted from ref.30.

is beneficial for the solar energy conversion efficiency, provided that a continuous path is maintained in each phase for the appropriate charge carrier to travel to the electrode ( fig.5.3a ). The concept of a bulk heterojunction is shown in fig.5.3. The schematic band structure displaying the HOMO and the LUMO of the materials and the work function of the electrodes are also illustrated.

Indeed, for solar cells the electron-hole pair(excitons)is generated by light in one of the polymers, usually the polymer with the narrowest band gap ( the absorber ), and diffuses to the polymer/polymer interface, where it can dissociate in to an electron and hole. The electron and hole are then separated and transported to

the opposite electrodes. In the context of the photodiodes, the polymer through which the electron is transported is often called the (electron) acceptor polymer, and the one that transports the hole the (electron)donor. The exciton generation has to happen in the vicinity of an interface, i.e, with in a distance comparable to the excitons diffusion length. The active region for photogeneration of excitons that can contribute to the current extends therefore only to 10nm from the polymer/polymer interface. An additional requirement for current generation is that the carriers can be collected efficiently at the electrodes, which means that the contacts should be ohmic. Ideally, the work function of the cathode should match the LUMO of the electron accepting polymer closely while the work function of the anode matches, the HOMO of the ( electron- ) donor polymer. This, together with the requirement that one electrode needs to be transparent, limits the choice of electrode materials. For intimately mixed blends, experimental results showed that only a few weight % of electron acceptor is sufficiently to quench virtually all excitations.

### 5.3 Characterization of photovoltaic devices

For the characterization of an organic photovoltaic cell; the following parameters are often used.

- Shortcircuit current ( $I_{sc}$ ):- This is the output current when the load impedance,  $R_L$  is much smaller than the device impedance. Ideally, the shortcircuit occurs when the  $R_L = 0$  so that  $V = 0$  in Eqn.5.2.2 and is equal to the current density,  $J_{ph}$ , generated by light, or

$$J = J_{sc} = J_{ph} \quad (5.3.1)$$

- open circuit voltage ( $V_{oc}$ ):-This is the voltage output when the load impedance much greater than the device impedance. Under open circuit condition,  $R_L$  approaches to  $\infty$  so that the net current is zero and the photocurrent is just balanced by the forward biased junction so we have

$$J = 0 = J_{ph} - J_o \left[ \exp\left(\frac{eV_{oc}}{nkT}\right) - 1 \right] \quad (5.3.2)$$

We can find the open circuit voltage,  $V_{oc}$  as

$$V_{oc} = \frac{nkT}{e} \ln\left(1 + \frac{J_{ph}}{J_o}\right) \quad (5.3.3)$$

A plot of the diode net current  $J$  as a function of the voltage  $V$  from Eqn. 5.2.2 is shown in fig.5.4. We may note the short circuit current and the open circuit voltage point on the fig.5.4.

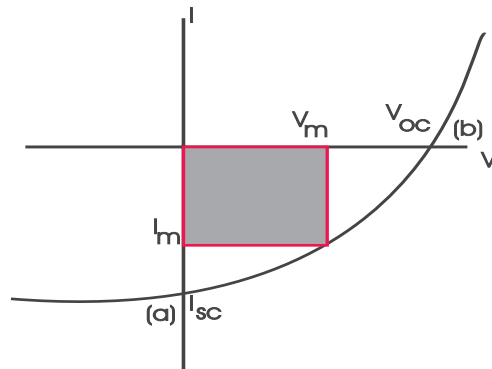


Figure 5.4: Maximum power rectangle of the solar cell I-V characteristics

- Maximum output power ( $P_m$ ) and Fill factor(FF). The power delivered to the

load is

$$p = IV = I_{ph}V - I_o[\exp(\frac{eV}{nkT}) - 1]V \quad (5.3.4)$$

where I is the net current output of the cell, and V is the voltage drop across the load. The current and voltage, which deliver the maximum power to the load can be found from Eqn. 5.3.4 by setting the derivative of p with respect to V equal to zero.

$$\frac{dp}{dV} = 0 = I_{ph} - I_o[\exp(\frac{eV_m}{nkT}) - 1] - I_oV_m(\frac{e}{nkT})\exp(\frac{eV_m}{nkT}) \quad (5.3.5)$$

Where  $V_m$  is the voltage which produces the maximum power. We may rewrite Eqn. 5.3.5 in the form

$$[1 + (\frac{e}{nkT})V_m]\exp(\frac{eV_m}{nkT}) = I + \frac{I_{ph}}{I_o} \quad (5.3.6)$$

The value of  $V_m$  and ( the value of the current at which  $V=V_m$  ) can be determined by trial error from the I-V curve of the cell under illumination. Fig.5.4 shows the maximum the maximum power rectangle of typical solar cell. A Fill factor or curve factor measures the quality of the solar cell as a power source and is defined as the ratio between the maximum power delivered to an external circuit and the potential power according to

$$FF = \frac{I_m V_m}{I_{sc} V_{oc}} \quad (5.3.7)$$

and is a number  $<1$ . Present high output inorganic solar cells have fill factor 0.6-0.7, but values up to 0.75 can be attainable.

- Monochromatic power conversion efficiency ( $\eta$ ):- It is the ratio of the maximum power from a solar cell of area A to the total power incident on the same device of area A.

$$\eta = \frac{\text{powerout}}{\text{powerin}} = \frac{I_m V_m}{p_{in}} \quad (5.3.8)$$

In general, the conversion efficiency of a solar cell in percentage is given by

$$\eta_{PCE} = \left( \frac{I_{sc} V_{oc}}{p_{in}} \right) FF \times 100\% \quad (5.3.9)$$

# Chapter 6

## Experimental

Samples were made both for optical-spectrophotometric and photovoltaic characterization. Samples for optical studies were made on glass substrate while for photovoltaic characterization were made on ITO coated glass.

### 6.1 Absorption spectrum measurement

Two types of chloroform solution were prepared to determine absorptions of the polymer for chloroform solution of pure PDOPT and PDOPT blended with PCBM in a 1:2 weight ratio with a concentration of 10 *mg/ml*. Each were prepared on separate glass substrate. The glass substrate was cut to the required size and washed with distilled water and ethanol successively. For the spin coating, the substrate was mount in the spin coater. The first spin coating was made by spinning pure PDOPT solution on the glass substrate, while the second using PDOPT blended with PCBM. All spinning processes were done using a programmable spinner system at a speed of 700rpm which yielded a thin uniform thin film. During spin coating process the solvent evaporates. Actually the thickness of the deposited polymer film can be controlled by the revolution and the concentration and the choice of the solvents. For a

given concentration of polymer solution, the higher the speed(rpm), the thinner the deposited film.

For optical absorption measurement thin film of the above shown in fig.6.1 was

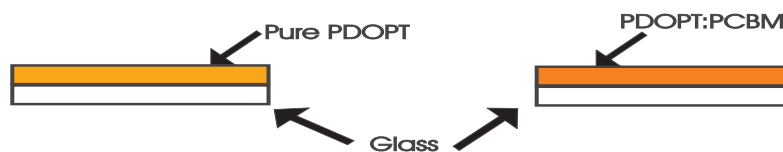


Figure 6.1: A polymer on the glass substrate prepared for Absorption

mounted on the sample holder of Perkin Elmer  $\lambda$  19UV/Vis/Nir spectrophotometer each one after the the other. The spectrophotometer is interfaced with the computer making use of software called UVCSS, ultraviolet computerized spectroscopy software. The absorption spectrum were obtained ( see the result and discussion section ) and analyzed.

## 6.2 Device preparation

The photovoltaic device of bulk hetrojunction solar cell was fabricated using PDOPT:PCBM (1/2,W/W ) as the active layer. The ITO (indium tin oxide) coated glass available in the laboratory were used. ITO is transparent and conductive and therefore often used as an electrode in PV and LEDs.

The ITO was structured by etching with an acidic mixture concentrated HCl : HNO<sub>3</sub> : H<sub>2</sub>O, 48 : 4 : 48 by volume for about 10 minutes. About two-third of the ITO/glass substrate was covered with a tape to protect the active ITO area against the etching acid. The etched part of of the ITO/glass provides a convenient region for electrical

contact to the aluminium layer deposited later. Then, the ITO/glass substrate was washed out successively with detergent, acetone, distilled water and finally rinsed with ethanol. The final clean glass plate with ITO one-third removed is as shown in fig.6.2. An aqueous solution conducting polymer poly ( ethylene dioxy thiophene



Figure 6.2: Diagram showing one-third of ITO is removed ready for spin coating

) -poly( styrene sulphonic acid )( PEDOT-PSS ) and PDOPT:PCBM were heated to remove possible entanglement that the polymer molecules may form. Finally the polymer relaxes the film forming capacity would increase. The PEDOT:PSS was spin coated on top of the well cleaned ITO/glass substrate at spin rate 3000 rpm. This was followed by annealing of the film at  $120^{\circ}C$  for 5 minutes, leaving a dried thin film. The PEDOT:PSS layer improves the quality of of the ITO electrode. The surface roughness of the ITO is minimized and the electric contact to the active layer is improved ( reduce the device leakage ). Further, the work function of the electrode is changed. Then, a chloroform solution of PDOPT:PCBM ( 1/2 ) weight ratio with concentration of  $10\text{ mg/ml}$  was spin coated on top of PEDOT:PSS at 700 rpm yielding thin film spread over the whole plate of as active layer. For electrical contact some part of the polymer film is removed from the etched part and the ITO part using acetone. Finally the low work function metal aluminium ( Al ) is thermally deposited partly on the active area film and partly on the clean glass. The deposition was done using Edward Auto 306 vacuum evaporator, at pressure in the chamber of the evaporator is reduced about  $7 \times 10^{-6} mB$ . As source, tungsten ( Molybdenum )

boats were used. The main purpose of reducing pressure in auto vacuum evaporator is to increase the mean free path ( the distance the aluminium atom can travel without collisions ) of aluminium atoms. Collisions may lead to chemical reactions between the metal and gas atoms ( oxide of aluminium); furthermore, the substrate and the film are bombarded by the gas atoms as well as by metal atoms. Both of these effects would lead to the contamination of thin film. In general, the better the the vacuum, lower the level of contamination. After aluminium is evaporated, the device was taken out of the chamber for characterization. The final sandwich type devices of bulk heterojunction solar cell of ITO/PEDOT-PSS/PDOPT:PCBM (1:2)/Al is depicted in fig.6.3.

During device preparation no special efforts were taken in reducing the moisture

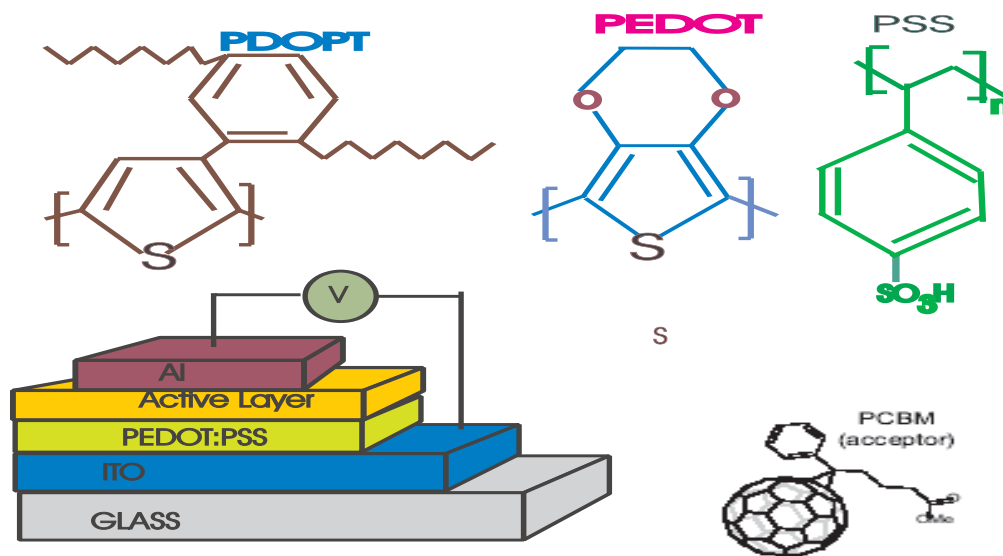


Figure 6.3: Finalized solar cell prepared for characterizations, Top: Chemical structure of PDOPT, PEDOT:PSS and PCBM

from the laboratory.

## 6.3 Device characterization

The sandwich structure shown in fig.6.3 provides a means for current-voltage and complex impedance measurement.

### 6.3.1 Current-Voltage measurement

The current-Voltage (I-V) characteristics in the dark, as well as under illumination was measured by using HP 4140B pA meter/DC voltage source, together with HP 16055A-test fixture. The measurement was taken by continuously sweeping the voltage applied from -3V to 3V at 10mV steps with hold time and step delay time of 1 Second. The I-V measurement under illumination was carried out by mounting inside the sample holder. The intensity of light incident on the cell was about  $100\text{mWcm}^{-2}$ . The plots of current density-voltage measurement (J-V) and lnJ-V curves are shown on fig.7.3 and 7.4.

### 6.3.2 Complex impedance measurement

Complex impedance spectroscopy of the device was measured as a function of frequency and applied bias voltage using HP 4192A LF impedance Analyzer together with an HP 16047A-test fixture. The data were taken at frequencies ranging from 0.5KHz to 40.5KHz for bias voltages ranging from -3V to 3V in steps of 1V. For every bias voltage, a sinusoidal oscillating voltage of  $V_{rms} = 50\text{mV}$  was used. Cole-Cole plot of the device is given in fig.7.6.

# Chapter 7

## Results and Discussion

### 7.1 Absorption spectra

The Absorption spectrum of PDOPT is shown in fig 7.1. It clearly indicates the broad spectral absorption region and some features of the vibronic states.

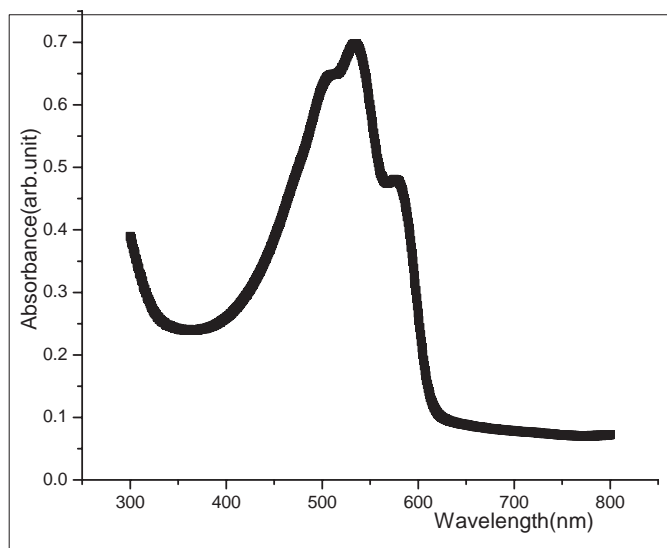


Figure 7.1: The Absorption spectrum of neutral PDOPT

This feature is the result of high order and reduced interchain interaction in PDOPT. The kink corresponding to higher energy( Left of the absorption peak ) is the energy

that absorbed when the vibration is out of phase and the one corresponding to lower energy( right of the peak ) is when the vibration is in phase.

The relatively low band gap suggest well order regions with extended conjugation

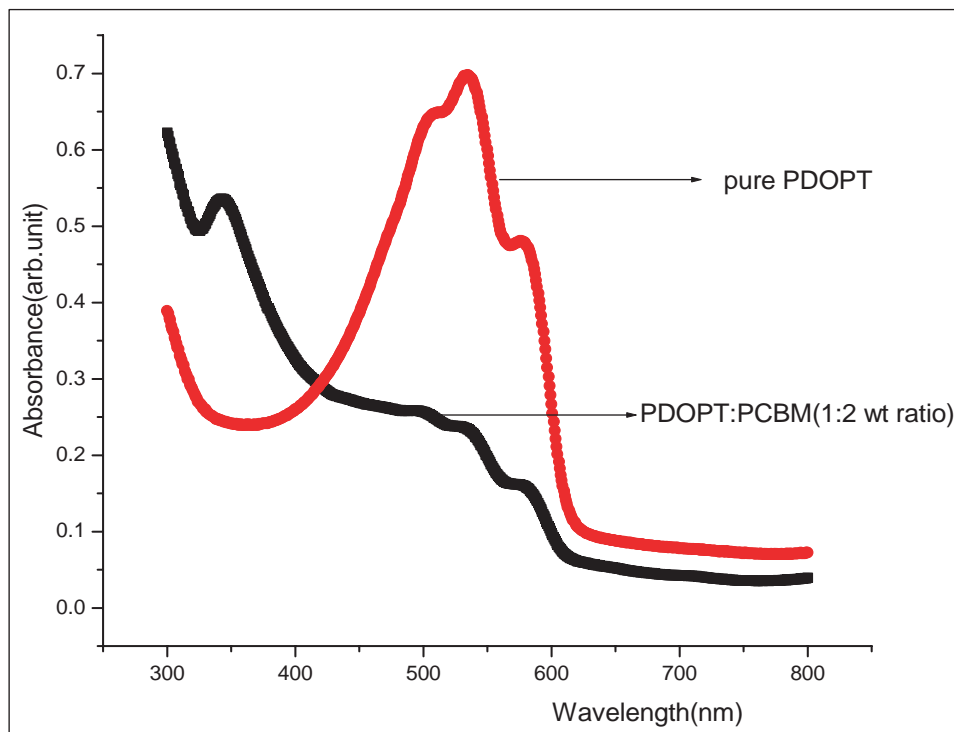


Figure 7.2: The Absorption spectrum of blend PDOPT:PCBM (1:2 Wt ratio) blend and pure PDOPT

along the polymeric back bone which is attributed to the increased interaction between the chains. The onset of absorption is at around 610 nm which corresponds to a band gap of 2.02eV. According to the absorption spectrum, a pure PDOPT polymer with such band gap can absorb light of wavelength in the range of visible light. This result is consistent with the previously reported observations[31]. Fig.7.2.shows the absorption spectrum of blend of PDOPT with fullerene derivative PCBM. The

absorption spectrum of PCBM in the visible region is not superposed with that of PDOPT. So we can have that the absorption spectrum of the composite have a minimized peak. This result confirms that there is a significant interaction between the two materials in the ground state.

## 7.2 Current density-Voltage ( J-V ) characteristics

The dark J-V curve of the bulk heterojunction device typically of ITO / PEDOT:PSS / PDOPT:PCBM / Al demonstrates typically rectifying diode like behavior. The forward bias corresponds to the Al being negative. The forward current increases exponentially at low forward bias voltage region and increases linearly at higher voltage regions. The rectification ratio,  $\gamma = 1.5 \times 10^3$  is determined. A semilogarithm plot (

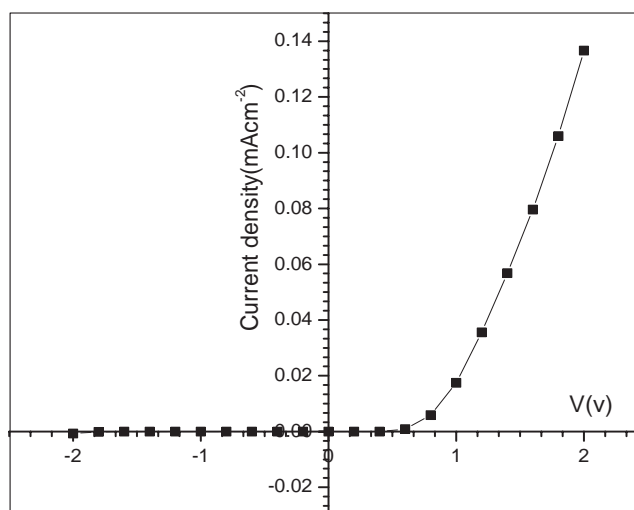


Figure 7.3: Current density-voltage characteristics of bulk heterojunction device of structure ITO/PEDOT:PSS/PDOPT:PCBM/Al

see fig.7.4 ) of the forward current density (  $J$  ) versus the applied voltage (  $V$  ) shows that the forward current increases exponentially with the applied voltage between 0.2V and 0.8V. This exponential dependence can be attributed to the formation of a depletion region between the aluminium and the active layer ( see also on the section on the Cole-Cole plot ). As it can also be observed in fig.7.4 that the current density deviates from its exponential dependence at the voltage higher than 0.8V. For such voltages higher than 0.8V, the current increase slowly i.e., the device unable to transport all the charges. Since a large amount of charges are injected in to the device. Hence, the growth of current is limited by the over all amount of charges loaded into the organic active layer thin film.

According to the Schottky barrier theory[8], p-type semiconductor forming a rectifying barrier at the interface when the work function of the metal is smaller than that of semiconductor. However, if the interface is formed between p-type semiconductor and a high work function metal the junction gives an ohmic J-V characteristics. In the Schottky barrier diodes, the J-V characteristics obey the well known Schottky equation and the dark current density is given by Eqn.4.1.1. The expression for  $J_o$  depends on how the charge transport is modelled. For the Schottky barrier devices the charge transport is usually assumed to be due to thermionic emission of the charge carrier over the potential barrier. The thermionic emission theory can be applied to this device and hence the current is assumed to be controlled only by the transfer of carriers across the Schottky interface.

For the voltage range between 0.2V and 0.8V the experimental data plotted as  $\ln J$  versus  $V$  fig.7.4 gives a linear curve; thus the term -1 in Eqn.4.1.1 can be neglected as  $\frac{qV}{nkT} \gg 1$ . The intercept of  $\ln J$  vs  $V$  on the vertical axis extrapolated backward will

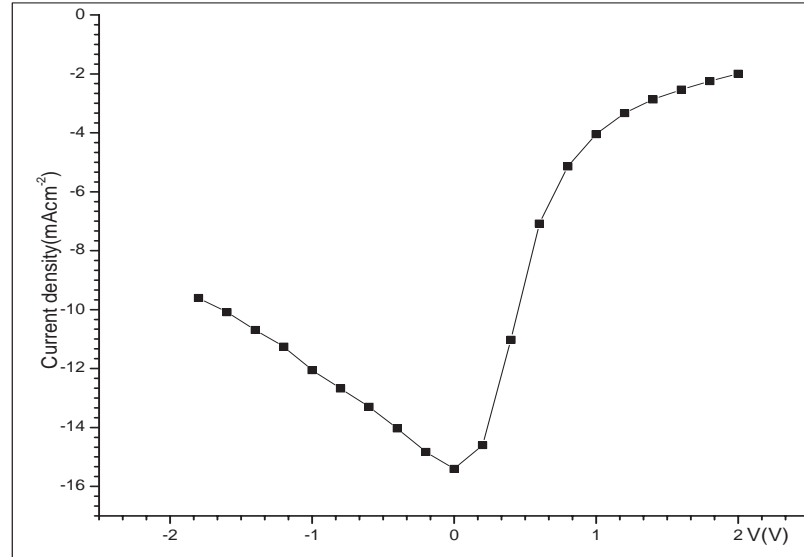


Figure 7.4: Semi-log plot of bulk heterojunction device of structure ITO/PEDOT:PSS/ PDOPT:PCBM/Al

give the saturation current density  $J_o$  and it was found to be  $1.0 \times 10^{-11} \text{ Acm}^{-2}$ . For The barrier height  $\Phi_b$  can be calculated from the value of  $J_o$  obtained and is found to be about 0.6V. The ideality factor,  $n$  of the device was obtained from the slop of the plot of  $\ln J$  vs  $V$  through the relation given by Eqn.4.1.5 The value of the ideality factor is thus  $n = 2.10$ . For an ideal diode,  $n=1$ . It is reported for Al/PDOPT/ITO that  $J_o$  and  $n$  are  $7 \times 10^{-11} \text{ Acm}^{-2}$  and 2.3 respectively[13]. So our result for the values of  $J_o$  and  $n$  are quite reasonable relative to the indicated values. The large value of ideality factor,  $n \geq 2$  was also observed and give an indication of (i) current crowding (ii) high probability of recombination of electrons and holes in the depletion region, and the occurence of tunnelling conduction[33]. The rectification ratio is also increase

Table 7.1: Electrical parameters extracted from the J-V characteristics in the dark

Parameter	$J_o$	$\Phi_b$	$\gamma$	n
Values	$1.0 \times 10^{-11} Acm^{-2}$	0.6V	$1.5 \times 10^3$	2.1

as we compare with the previously reported observation[13]. The electrical parameters obtained from the J-V measurements are summarized as in Table7.1.

The J-V characteristics of this device under  $100mWcm^{-2}$  white light illumination through the transparent conducting electrode ITO side is given in fig.7.5. According to the curve, the device shows photovoltaic behavior. From the measured J-V

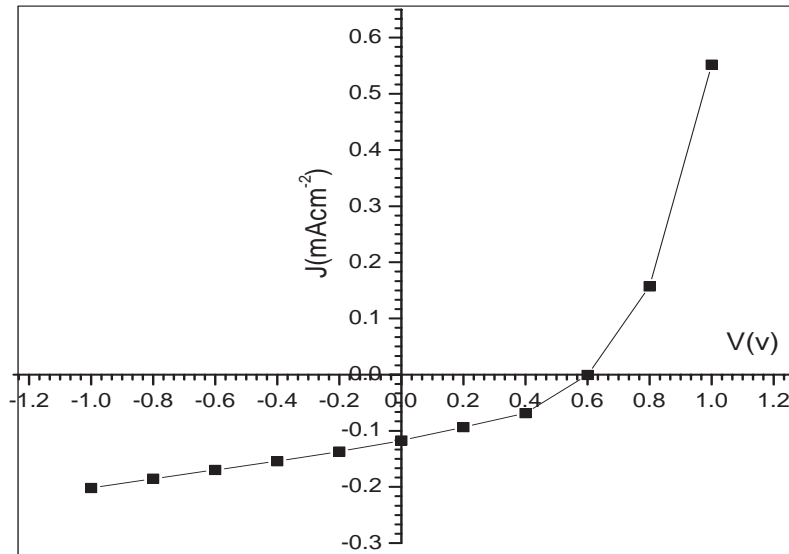


Figure 7.5: J-V characteristics of bulk heterojunction device of structure ITO/ PE-DOT:PSS/ PDOPT:PCBM/Al under illumination of  $100mWcm^{-2}$

curve, the open circuit voltage ( $V_{oc}$ ), short circuit current density ( $J_{sc}$ ), fill factor (FF), and power conversion efficiency were calculated and are given in Table 7.2. The efficiency is quit poor. The poor efficiency of this device and any organic bulk

Table 7.2: Photovoltaic performance parameters of bulk heterojunction solar cell device under  $100mWcm^{-2}$  illumination

Active layer	$J_{sc}(mAcm^{-2})$	$V_{oc}(mV)$	FF	$\eta(\%)$
PDOPT:PCBM(1/2,W/W)	0.1174	600	0.4	0.028

heterojunction solar cell could explained as follows: Heterojunctions work very well at separating excitons that arrive at the junctions. Unfortunately the life time of excitons is short, thus, only excitons that are formed within  $\sim 10nm$  of the junction will ever reach the electrodes. This short diffusion length of excitons clearly limits the short circuit current density as well as the efficiency of the photovoltaic devices. So the the thickness of such a devices should be small enough to make all the excitons reach the interface and have a maximum efficiency from such device.

The photovoltaic efficiency of such device also depends on the absorption of the incident photon and transfer of the free charge carriers ( mobility ) to the external circuit. Most of the conjugated polymers including PDOPT have a high mobility for holes in the undoped form and it hinders the effective transfer of electrons to the electrodes. The interpenetrating networks and heterojunctions which are made by blending the polymer with fullerene lack high transfer rates which results in low efficiency and higher recombination rate due to high density of photoinduced free carriers. It is also to be noted that eventhough the charge transfer process at the interfaces happens within nanoseconds, the transport property of the acceptor molecule PCBM is poor, which results in low transfer of free charge carriers to the electrode. This also increases the recombination rate. Such problems can also be overcome by blending the polymer other than PCBM which is intrinsically electron transporting and has

the energy levels which can form a pn-hetrojunction similar to the inorganic one[29]. As we could observe in the fig.7.2 or 7.1. of the absorption profile is not broad enough to match the solar spectrum; So it was found to be difficult to extract a very high photocurrent. To alleviate this problems it is necessary to design the polymers by blending in appropriate geometry or else to tune the band gap of the active component of the polymer, PDPOT using substituent effects[Christoph et al]. Inorder to increase the efficiency of the PV device made with our polymer one possible suggestion would be to blend it with other polymer having low band gap (  $E_g < 1.8\text{eV}$  ). In this way, we will be able to expand the spectral region of bulk heterojunction solar cell. Thus, we could enhance the spectral photon harvesting. Since blending to polymers with similar wavelength range of absorption does not help much to cover the broad solar spectrum.

The most efficient devices reported on using chlorobenzene as a solvent and have a large fullerene content up to 80% by weight for different blends of MEH-PPV:PCBM showed increased mobility upon increasing the content of the PCBM. For charge generation, a few percent would be sufficient. But the interconnection of all acceptor ( PCBM ) molecules in the bulk is of importance for efficient charge collection. Isolated fullerene molecules or clusters are charge traps and the electrons are captured there. Hence, blend ratio can also be factor for a very low efficiency of this bulk hetrojunction solar cell. On the other hand both photocurrent generation and charge transport are functions of morphology[30].

$V_b$	$R_c(\Omega)(\pm 10)$	$R(K\Omega)$	$C(nF/cm^2)$
-2	115	17.4	40
-1	115	26.6	57
1	115	22.2	48
2	115	9.7	60

Table 7.3: Parameters obtained from the impedance spectra for the device under test

### 7.3 The Cole-Cole plot

Fig.7.6 shows the result of the impedance measurements across the electrode of the formed diodes, as a function of frequency and applied voltage. The real and complex parts of the impedance  $Z_{real}$  and  $Z_{imag}$  were recorded at a test frequency between 0.5Kz and 40.5KHz at a range of different applied biases. All of the  $Z_{imag}$  versus  $Z_{real}$  results at different biases showed a single semicircle which are consistent with the J-V measurements results under dark. This single semicircle in the Cole-Cole plots was found to be displaced slightly along the  $Z_{real}$  axis away from the origin. This can be associated with small resistance  $R_c$  of the order of 0.1-0.13  $K\Omega$  placed in series to the main parallel RC network.

As it can be seen in the fig.7.6 the semicircles are bias voltage dependent. So we can model our sample by an equivalent circuit given in fig.7.7 below.

The arrows indicate that both R and C are bias voltage dependent. The relation  $Z_{imag} = (\omega C)^{-1}$  is used to estimate the value of the capacitance C. Knowing  $f$  ( $\omega = 2\pi f$ ) and  $Z_{imag}$  gives the value of C for the corresponding bias voltage. The parameters from the Cole-Cole plot are listed in Table 7.3. The diameter of these semicircles corresponds to the resistance of the depletion region. The Cole-Cole plot depicts the

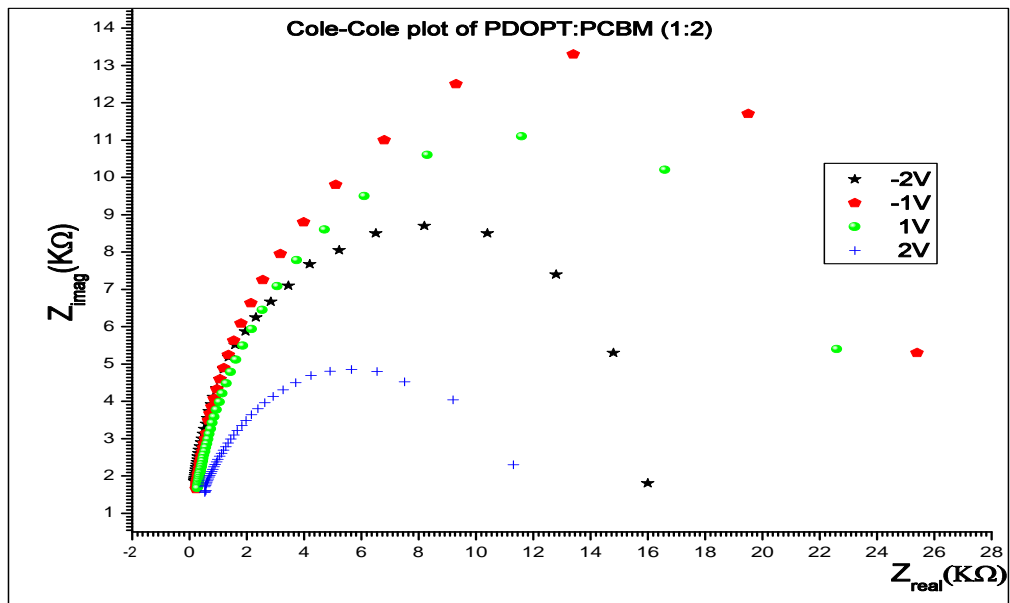


Figure 7.6: Cole-Cole plots of bulk heterojunction device of structure ITO/PEDOT:PSS/ PDOPT:PCBM/Al

smallest at +2V indicating the resistance is low and increase at the intermediate small bias voltages. This is reasonably consistent with the dark J-V results shown in fig.7.3.

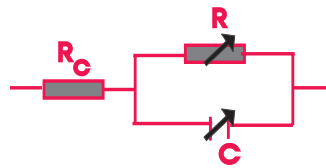


Figure 7.7: An equivalent circuit for the device under test as model for the Cole-Cole plot of fig 7.6

# Conclusion

In this work we studied the property of the photovoltaic (PV) devices whose active layer is made from the p-type, PDOPT and n-type, PCBM polymer blend. The PV cell has sandwich type structure, ITO/PEDOT:PSS/PDOPT/Al . The device showed typical photovoltaic behavior. The J-V characteristics were studied using thermionic emission theory. However, the Schottky model used here only as a first approximation. For small forward bias voltages, the J-V characteristics is governed by the thermionic emission theory. However, for higher voltages the resistance of the depletion region decreases and ohmic behavior as well as space charge limited current dominates. The interface between the Aluminium and the polymer blend as evidenced by the Cole-Cole plot manifests part of single semicircles which is bias dependent. It has also shown slight increase of the resistance of the depletion layer at smaller magnitudes of bias voltage. This is a confirmation for the existence of tunnelling conduction. Photovoltaic performance parameters in particular  $J_{sc}$  and  $\eta$  % was found to indicate low in magnitude that is  $0.1174 \text{ mAcm}^{-2}$  and  $0.028$  % respectively. These resulted from low absorption of the active layer as well as the mismatch of optical absorption of the material ( PDOPT:PCBM ) and the solar spectrum.

Further studies are therefore necessary to get a device with high performance parameters with such polymer by tuning its band gap or blending with material absorbing

in infrared (IR) or near IR region.

# Bibliography

- [1] Rolf E.Hummel Electronic properties of Materials, 2nd ed., Springer-Verlag 1993.
- [2] K.J.Saunders, Organic Polymer Chemistry 2nd., Chapman and Hall Ltd 1988.
- [3] David I. Bower, Introduction to Polymer physics.Cambrdge university press.(2002).
- [4] Ellen Moons, J.Phys.: Condens. Matter **14** (2002)12235-12260, IOP publishing Ltd.
- [5] E.Kymakis, E Koudoumas, I Franghiadakis and G A J Amaratunga. J. phys.D: Appl.phys. **39** (2006)1058-1062 IOP publishing Ltd.
- [6] W.Bantikassegne, PhD Disertation, ISBN 91-7871-581-4, Linkoping university, Sweden, 1996.
- [7] Richard H. Hube. Electronics in Solids: An introductory survey. 3rd ed., Academic press, Inc. London, 1990.
- [8] Donald A. Neamen, Semiconductor physics and Devices: Basic principles. Richard D.Irwin, Inc., Boston, 1992.
- [9] A B Kaiser. Rep. Prog. Phys. **64** (2001).

- [10] T. Granlud. PhD Dissertation, ISBN 91-7219-733-1, Linkoping university, Sweden, 2000.
- [11] William R.Salaneck. Organic electronics, Part-I: From molecules to Materials. Linkoping 2002-09-19.
- [12] N. W. Aschcroft and N.D.Mermin, Solid State Physics,Holt,Rinehat and Winston, N.Y.,(1976).
- [13] T. Getachew,Msc Thesis,Department of physics, AAU (2001).
- [14] Chiang, C.K.,Fincher, C.R., Park, Y.W., Heeger,A.J.,Shirakawa, H.,Lois, E.J., Gau,S.C, MacDiarmid, A.G. Phys.Rev. Lett, 1997, **39**, 1098.
- [15] Dipl.Ing. Klaus Petrtsch. PhD Thesis, Cambridge and Graz, July 2000.
- [16] Joakim Isaksson. Electrochemical switching of color and wettability in conducting polymers derivatives. Linkoping universitet institute of technolgy. ISBN: 91-85457-28-0. Sweden, 2005.
- [17] Jean-Pierre Farges. Organic conductors: Fundamentals and applications. Marcel Dekker, Inc. Newyork, 1994.
- [18] S.Kivelson,Phys.Rev.Lett., **46** (1981)1344.
- [19] Jan Przyluski. Sold state phenomena: Conducting polymer-Electrochemistry. Vol. 13& 14 Sci-Tech pub. Ltd 1990.
- [20] A.B Walker, A Kambili and S.J Martin. J. Phys,,: Condens. Matter **14** (2002).
- [21] S.M.Sze. Physics of Semiconductor Devices, 2nd ed., John wiley & sons,1981.

- [22] C.J. Brabec, N.Serdar Sariciftci, and Jan C. Hummelen. *Adv.Fun. Mater.* **11** 2001.
- [23] Donald A. Seanor. *Electrical properties of Polymers*. Academic press, Inc. 1982.
- [24] Jovan Mijovic and Francesco Belluci. *Trip* Vol. **4** No.3 (1996).
- [25] J.R. MacDonald,ed., *Impedance spectroscopy Emphasizing Solid materials*, John wiley & sons, Newyork, (1987).
- [26] Serdar Niyanzi Sariciftci, Christoph Winder, Christoph Brabec. *Sensitization of Low band gap polymer Bulk hetrojunction solar cells*. Universitat Linz. sep 2001.
- [27] Christoph Winder and Niyazi serdar Sariciftci. *J. Mater. chem.* **14** (2004).
- [28] H. Hoppe and Niyazi Serdar Sariciftci. *J. Mater.Res.*, Vol. 19, No.7 July 2004.
- [29] I.D Parker. *J. Appl.phys*, **75**,1656(1994).
- [30] Christoph J. Brabec,N. Serdar Sarciftici, and Jan C. Hummelen. *Adv. Funt. Mater.* **11**(1) 2001.
- [31] G.Goro. Msc Thesis, Department of physics, AAU (1998)
- [32] Lucimara S. Roman, Mats R. Andersson, Teketel Yohannes, and Olle Inganas. *Adv. Mater.* 1997, 9, No.15.
- [33] J. KAnicki, in T.A Skotherim ( ed.), *Handbook of Conducting Polymers*, Vol.1, Marcel Dekker,1986.